A Physics-Based Emissions Model for Aircraft Gas Turbine Combustors

by

Douglas L. Allaire

Submitted to the Department of Aeronautics and Astronautics
in partial fulfillment of the requirements for the degree of

Master of Science in Aerospace Engineering

at the

MASSACHUSETTS INSTITUTE OF TECHNOLOGY

May 2006

Author .....
Department of Aeronautics and Astronautics
May 26, 2006

Certified by .....
Karen Willcox
Associate Professor
Thesis Supervisor

Certified by .....
Ian Waitz
Professor
Thesis Supervisor

Accepted by .....
Jaime Peraire
Professor of Aeronautics and Astronautics
Chairman, Department Committee on Graduate Students

A Physics-Based Emissions Model for Aircraft Gas Turbine Combustors

by

Douglas L. Allaire

Submitted to the Department of Aeronautics and Astronautics
on May 26, 2006, in partial fulfillment of the
requirements for the degree of
Master of Science in Aerospace Engineering

Abstract

In this thesis, a physics-based model of an aircraft gas turbine combustor is developed for predicting NO_x and CO emissions. The objective of the model is to predict the emissions of current and potential future gas turbine engines within quantified uncertainty bounds for the purpose of assessing design tradeoffs and interdependencies in a policy-making setting. The approach taken is to capture the physical relationships among operating conditions, combustor design parameters, and pollutant emissions. The model is developed using only high-level combustor design parameters and ideal reactors. The predictive capability of the model is assessed by comparing model estimates of NO_x and CO emissions from five different industry combustors to certification data.

The model developed in this work correctly captures the physical relationships between engine operating conditions, combustor design parameters, and NO_x and CO emissions. The NO_x estimates are as good as, or better than, the NO_x estimates from an established empirical model; and the CO estimates are within the uncertainty in the certification data at most of the important low power operating conditions.

Thesis Supervisor: Karen Willcox
Title: Associate Professor

Thesis Supervisor: Ian Waitz
Title: Professor

Acknowledgments

The work presented in this thesis was possible because of the technical support provided by a number of people. To all of these people I owe a great deal of thanks. First and foremost, I would like to thank my advisors, Prof. Karen Willcox and Prof. Ian Waitz. Their assistance and guidance in the technical aspects of this work was crucial to its completion. I would also like to thank Joe Palladino, who provided me with expert knowledge of the aircraft engine industry and every bit of data that I thought could help with the research. I also received a great deal of help from industry that made this research possible. For this I would like to thank Frank Lastrina and Hukam Mongia from General Electric and Nan-Suey Liu from NASA Glenn. A great deal of thanks is also owed to Sean Bradshaw and Steve Lukachko for handling all of the questions I asked them along the way with patience and a genuine interest in helping me get a handle on combustion and to Garrett Barter, who guided me through several computer related issues that would have taken me weeks to figure out on my own.

Finally, I would like to thank my friends and my family for their support during this research and throughout my life.

Contents

1 Introduction **15**

1.1 Motivation for Emissions Prediction 15

1.1.1 Major Aircraft Engine Emissions 16

1.1.2 The ICAO Regulation Process 18

1.1.3 An Emissions Tool for Trade Studies 19

1.2 Necesssary Attributes of an Emissions Model for Policy Making . . . 21

1.3 Current Emissions Prediction Strategies and Techniques 21

1.3.1 Empirical Models 21

1.3.2 Semiempirical Models 24

1.3.3 Simplified Physics-Based Models 25

1.3.4 High Fidelity Simulations 25

1.3.5 State of the Art for Emissions Trade Analyses 26

1.4 A Physics-Based Emissions Model 27

1.4.1 Objective 27

1.4.2 Emissions Model Success Criteria 27

1.5 Thesis Outline 28

2 Developing a Physics-Based Emissions Model **29**

2.1 Functional Requirements 29

2.2 Model Input/Output 30

2.3 Combustion Fundamentals 30

2.4 Governing Equations 31

2.5 Reducing the Governing Equations 32

2.5.1 The Perfectly Stirred Reactor 32
2.5.2 PLUG Flow Reactor 35
2.6 Modeling a Gas Turbine Combustor with Ideal Reactors 36
2.6.1 The Role of the Primary Zone 36
2.6.2 Modeling the Primary Zone 37
2.6.3 Primary Zone Emissions Considerations 37
2.6.4 Assumptions and Limitations of the Primary Zone Model . . . 41
2.6.5 The Role of the Intermediate Zone 42
2.6.6 Modeling the Intermediate Zone 42
2.6.7 Intermediate Zone Emissions Considerations 44
2.6.8 Assumptions and Limitations of the Intermediate Zone Models 44
2.6.9 The Role of the Dilution Zone 44
2.6.10 Modeling the Dilution Zone 44
2.6.11 Modeling the Injection of Dilution/Cooling Air 45
2.6.12 Assumptions and Limitations of Injection Mapping 46
2.6.13 Model Implementation 47
2.6.14 The Physics-Based Emissions Model 47

3 Setting the Unmixedness Parameter **49**
3.1 Industry Data 50
3.2 Sensitivity to Unmixedness 50
3.2.1 Single Value Optimization 50
3.2.2 General Curve Optimization 52
3.2.3 Individual Curve Optimization 54
3.3 Evaluating the Different Options 55
3.3.1 Single Point Estimate 55
3.3.2 General Curve Estimate 56
3.3.3 Individual Curve Estimate 56
3.4 Setting Unmixedness 57
3.5 Unmixedness Parameter Issues 57

4 Assessing the Predictive Capability of the Model **61**

4.1 NO_x Chemistry 61

4.2 CO Chemistry 63

4.3 Predicting NO_x and CO Chemically 64

4.4 Model Response to T_3 64

4.5 Model Response to P_3 66

4.6 Model Response to Equivalence Ratio 68

4.7 Capturing the Effects of Gas Turbine Combustor Design 70

4.7.1 Idle Emissions Output 70

4.7.2 Approach Emissions Output 71

4.7.3 Climb-Out Emissions Output 73

4.7.4 Takeoff Emissions Output 73

4.7.5 Assessment of Model Capability 75

5 Results **77**

5.1 Model Predictions for Engines 1, 2, and 3 77

5.1.1 Overview of the Results 78

5.1.2 Engine 1 Estimates 78

5.1.3 Engine 2 Estimates 80

5.1.4 Engine 3 Estimates 80

5.1.5 Overall Estimates 83

5.1.6 Discussion of Engine 1, 2, and 3 Model Estimates 84

5.2 Predicting the Effects of Design Changes 84

5.2.1 Overview of Results 84

5.2.2 Engine 1a to Engine 1 85

5.2.3 Discussion of the Engine 1a to Engine 1 Design Change Results 88

5.2.4 Engine 3 to Engine 3a 89

5.2.5 Discussion of the Engine 3 to Engine 3a Design Change Results 92

5.3 NO_x Estimates for a Full Throttle Sweep 93

5.3.1 Throttle Sweep Emissions Estimates 93

5.3.2 Throttle Sweep Estimates versus Boeing Fuel Flow Method 2 . 94

6 Conclusions and Future Work **97**

6.1 Conclusions 97

6.2 Future Work 100

List of Figures

1-1 Regional NO_x Emissions in the US [7] 17

1-2 Radiative Forcing from Aircraft [9] 18

1-3 ICAO LTO Cycle [8] 19

1-4 NO_x Emissions by Combustor Technology Generation [10] 20

2-1 Diagram of a Perfectly Stirred Reactor, adapted from [17] 33

2-2 Diagram of a Plug Flow Reactor, adapted from [17] 35

2-3 The Effect of Turbulence on Damkohler Number [18] 38

2-4 Normal Distribution of Equivalence Ratio in the Primary Zone PSRs 39

2-5 Determining the Primary Zone Model 40

2-6 Diagram of the Primary Zone Model 41

2-7 Diagram of the Intermediate Zone Model 43

2-8 Diagram of the Dilution Zone Model 45

2-9 Typical Combustor Flow Splits 46

2-10 Diagram of the Physics-Based Emissions Model 47

3-1 Response of Engine 1a Emissions to Varying Unmixedness 51

3-2 Unmixedness versus Primary Zone Equivalence Ratio [19] 53

3-3 Model Unmixedness versus Primary Zone Equivalence Ratio 54

3-4 Model Unmixedness versus Primary Zone Equivalence Ratio for LTO Cycle 55

4-1 Model $EINO_x$ versus Combustor Inlet Temperature 65

4-2 Model EICO versus Combustor Inlet Temperature 66

4-3 Effect of Pressure on Flame Temperature, adapted from [14] 67
4-4 Model $EINO_x$ versus Combustor Inlet Pressure 67
4-5 Model EICO versus Combustor Inlet Pressure 68
4-6 Model $EINO_x$ versus Primary Zone Equivalence Ratio 69
4-7 Model EICO versus Primary Zone Equivalence Ratio 70
4-8 Model Combustor Zone Emissions Production at Idle Power 71
4-9 Model Combustor Zone Emissions Production at Approach Power . . 72
4-10 Carbon Monoxide Emissions versus Primary Zone Equivalence Ratio [14] 73
4-11 Model Combustor Zone Emissions Production at Climb Out Power . 74
4-12 Model Combustor Zone Emissions Production at Takeoff Power . . . 74

5-1 Emissions Estimates for Engine 1 79
5-2 Emissions Estimates for Engine 2 81
5-3 Emissions Estimates for Engine 3 82
5-4 Emissions Estimates for Engines 1, 2, and 3 83
5-5 Percentage Change of Inputs from Engine 1 to Engine 1a 89
5-6 Percentage Change of Inputs from Engine 3 to Engine 3a 92
5-7 Throttle Sweep Emissions Estimates for Engine 1a 94
5-8 Throttle Sweep Emissions Estimates for Engine 1a Compared with Boeing Fuel Flow Method 2 95

List of Tables

1.1 Full Simulation Time [15] 26

3.1 Relative Power of Each Engine in the Study 50
3.2 Single Value Optimized Unmixedness 52
3.3 Comparison of Engine 1 Calculated and Optimized Unmixedness . . . 56
3.4 Comparison of Engine 1a Calculated and Optimized Unmixedness . . 56
3.5 Comparison of Engine 1a Calculated and Optimized Unmixedness . . 57
3.6 Comparison of Engine 1a Calculated and Optimized Unmixedness . . 59

5.1 Engine 1a NO_x Emissions 85
5.2 Engine 1a CO Emissions 86
5.3 Engine 1 NO_x Emissions 86
5.4 Engine 1a and Engine 1 NO_x Dp/Foo Estimates 87
5.5 Engine 1 CO Emissions 87
5.6 Engine 1a and Engine 1 CO Dp/Foo Estimates 88
5.7 Engine 3 NO_x Emissions 90
5.8 Engine 3 CO Emissions 90
5.9 Engine 3a NO_x Emissions 91
5.10 Engine 3 and Engine 3a NO_x Dp/Foo Estimates 91
5.11 Engine 3a CO Emissions 91
5.12 Engine 3 and Engine 3a CO Dp/Foo Estimates 92

Chapter 1

Introduction

Increasing concern over local air quality, community noise, and climate change caused by air transportation has led to an effort aimed at developing a means to articulate trade-offs at the aircraft design level among fuel burn, emissions of local air quality pollutants, cruise emissions, and community noise. A tool, called the Environmental Design Space (EDS), is therefore being created, which is intended as an aircraft system level design tool for use in regulatory policy making within the FAA and the International Civil Aviation Organization (ICAO). A critical aspect of EDS is the development of an emissions model capable of capturing the interdependencies between different emissions, noise, and engine performance. The development of such an emissions model is the topic of this thesis.

1.1 Motivation for Emissions Prediction

The worldwide fleet of aircraft is expected to more than double in the next twenty years [1]. Development of new technology is not expected offset the increase in emissions caused by the growth in aviation [2]. Due to a lag in the introduction of technology in the aviation industry, the time required to transition from basic research to fleet impact can be as much as 25 years [3]. Because of this, a method is desired for assessing the influence of different policy scenarios regarding trade-offs on engine emissions and other aircraft design parameters.

1.1.1 Major Aircraft Engine Emissions

Emissions from aircraft engines that impact local air quality are oxides of nitrogen, carbon monoxide, soot, unburned hydrocarbons, and oxides of sulfur. Oxides of nitrogen, commonly referred to as NO_x, consist of NO and NO_2, and are the most highly regulated pollutants from aircraft engines [4]. NO_x emissions also tend to be difficult to control because changes in engine design aimed at improving fuel efficiency often make it more challenging to limit NO_x production. Between 1970 and 1998 for example, emissions of all major aircraft pollutants except for NO_x, decreased, while NO_x emissions increased by about 10% [5].

Carbon monoxide, known as CO, is another regulated emission. According to work done by Lukachko and Waitz however, the impact of aviation CO on the environment is only about $1/100^{\text{th}}$ of the impact of NO_x emissions [6]. Even so, CO emissions are regulated and need to be accounted for by an emissions prediction model.

While there are other important emissions from aircraft engines, in particular soot, this thesis focuses only on modeling the gaseous emissions, NO_x and CO.

Local NO_x Emissions

Both NO_x and CO emissions are regulated because of their effects on the environment and on human health. The effects of CO are mainly local, while the effects of NO_x are felt both locally and globally. As shown in Figure 1-1, in 1999 it was predicted that by 2010 there would be significant increases in regional NO_x produced by aircraft relative to what was being produced in 1990. Worldwide low altitude NO_x emissions from aircraft are expected to increase by a factor of 2.6 between 2002 and 2020 [5]. These anticipated increases in NO_x are of concern because of the health issues associated with local NO_x production, in particular the production of ground-level ozone (smog), which can lead to respiratory problems and other detriments to human health.

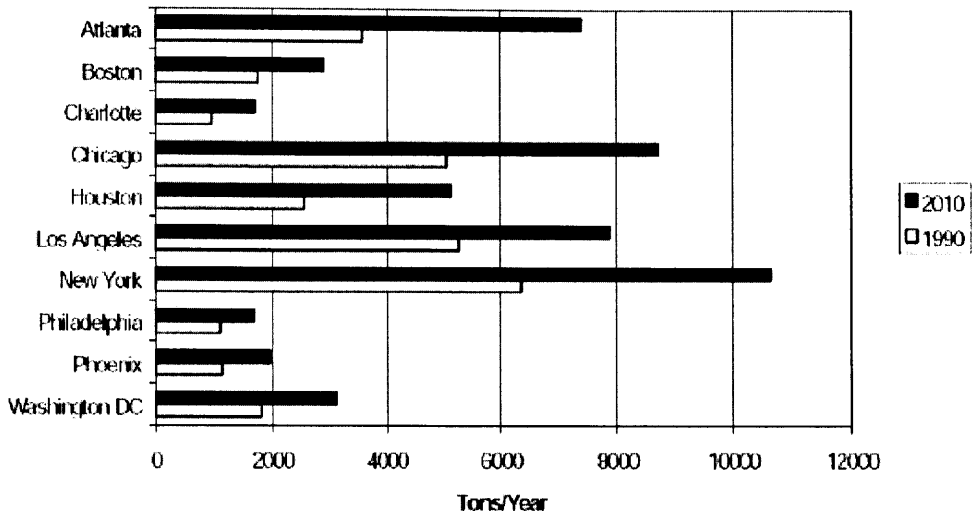

Figure 1-1: Regional NO_x Emissions in the US [7]

Local CO Emissions

CO has been reduced by operating at nearly 100% combustion efficiency at high power settings. While taxiing on airport runways, however, combustors do not operate as efficiently and higher levels of CO are produced. Carbon monoxide emissions caused by idling aircraft engines in airports are a health concern because CO reduces the oxygen carrying capacity of blood and significantly reduces the ability of a person to perform physical activities.

Cruise Emissions

As mentioned previously, NO_x emissions also have a global effect. This is because at cruise altitude, emissions of NO_x contribute to the formation of atmospheric ozone and the depletion of atmospheric methane. Significant NO_x emissions injected directly into the upper troposphere/lower stratosphere, may lead to climate change. Figure 1-2 shows the estimated contributions to radiative forcing of aircraft emissions in 1992 as well as a projection to 2050. Radiative forcing essentially means the approximate global effect on climate and the labels: good, fair, poor, refer to the level of understanding of the effect. The whiskers on the figures are the 67% confidence

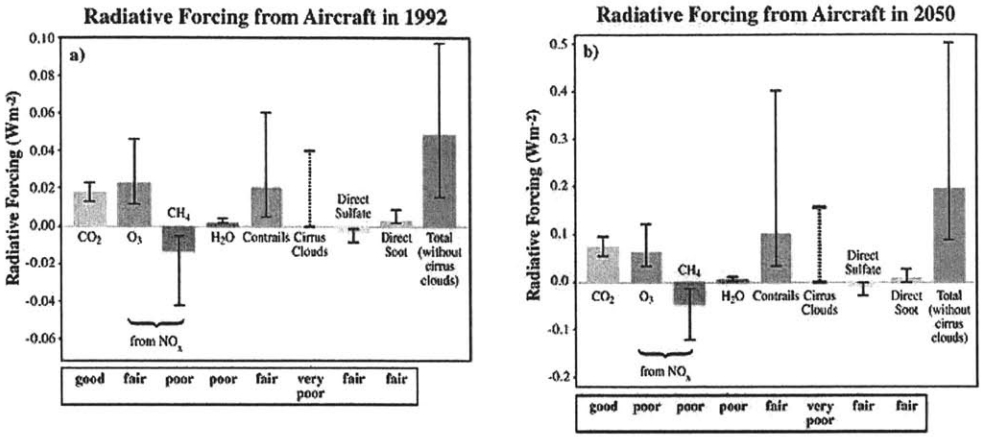

Figure 1-2: Radiative Forcing from Aircraft [9]

limits. The 2050 projection has a scale that is about a factor of five different from the scale in 1992, showing that the effects of aircraft emissions on the global climate are expected to increase. For this reason policies to control cruise emissions are being considered and an emissions model should be capable of predicting aircraft engine emissions at all engine settings.

1.1.2 The ICAO Regulation Process

The International Civil Aviation Organization, (ICAO), determines the emissions regulations to be met by all subscribing countries. The method the ICAO uses is based only on the landing-takeoff cycle (LTO cycle). The LTO cycle is shown in Figure 1-3, where idle is 7% sea level static (SLS) thrust, approach is 30%, climb out is 85%, and takeoff is 100% SLS thrust. Engines are certified based on time in mode (TIM), which is defined in Figure 1-3, emissions index (EI), fuel flow rate ($\dot{m}_f$), and rated output (RO). An emissions index is defined as the ratio of grams of a particular pollutant to kilograms of fuel burned. The certification variable for each pollutant is in the form of a Dp/Foo, which is defined as

$$\text{Dp/Foo} = \sum_{i=1}^{4} \text{EI}_i \times \text{TIM}_i \times \dot{m}_{f_i}/\text{RO}, \tag{1.1}$$

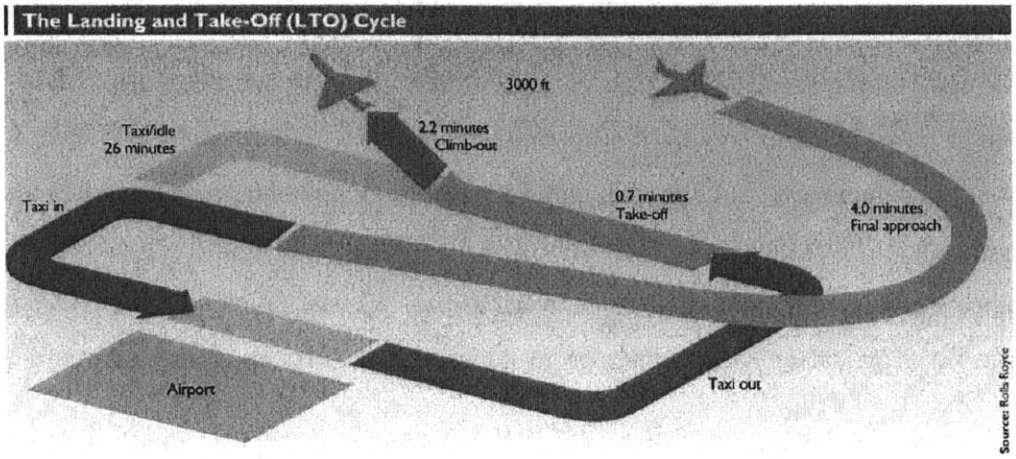

Figure 1-3: ICAO LTO Cycle [8]

where the sum is over the four ICAO LTO-cycle points. The most recent regulation on NO_x emissions from the ICAO is

$$\text{LTO } NO_x = -1.0 + 2 \cdot \text{OPR}, \tag{1.2}$$

where OPR refers to the overall pressure ratio of the engine being certified. The regulation is for engines with OPRs between 30 and 82.5 and places a linear barrier on the maximum Dp/Foo allowable for NO_x.

The ICAO currently does not have a non-proprietary, physics-based capability for looking at trade-offs for different emissions under different regulatory policy scenarios. Therefore, well-intended actions to improve emissions of a particular pollutant, can lead to unintended negative impacts on other emissions, noise, or engine performance. The purpose of the emissions modeling methods described in this thesis is to estimate the design trade-offs and the effects of design changes on emissions so that these trade-offs can be more rigorously estimated during the analysis of potential policy changes.

1.1.3 An Emissions Tool for Trade Studies

Over the past 40 years, fuel consumption for commercial aviation aircraft has been reduced by 70%, noise has been reduced by 50%, and CO and unburned hydrocarbons

(UHC) have been reduced by about 90% [5]. These improvements have come from the ability to increase OPR, bypass ratio, and turbine entry temperature (TET), due to better materials and cooling methods, which leads to higher thermal efficiency and combustion efficiency. During this same time period however, as previously noted, NO_x emissions have risen approximately 10% for commericial aviation aircraft. Figure 1-4 shows four generations of engines over the past 30 years plotted with NO_x versus engine pressure ratio. The change from generation 1 through 4 saw an increase in

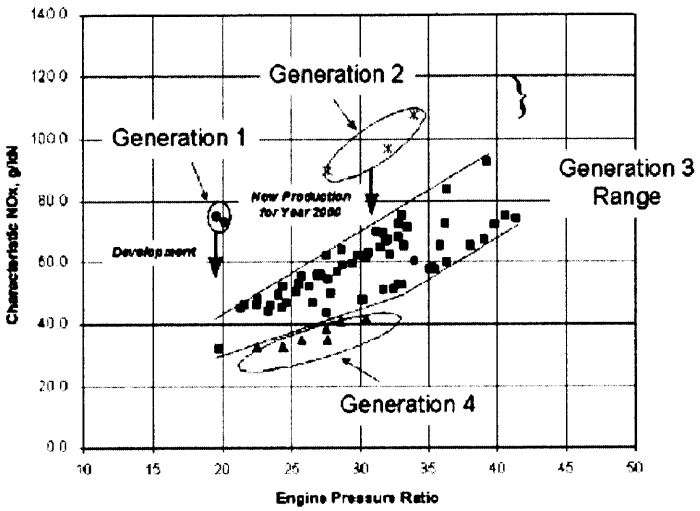

Figure 1-4: NO_x Emissions by Combustor Technology Generation [10]

pressure ratio from 20 to 40 and an increase in the TET. The combined effect of these changes led to an increase in thermal efficiency from 48% to 55% but it also led to some of the generation 3 engines, which make up most of the engines in the current aircraft fleet, with NO_x levels similar to the generation 1 engines [10]. Assessing such trade-offs among different emissions, fuel burn, and noise is essential, and to do this, an emissions model must exist that has the ability to take part in trade studies.

1.2 Necesssary Attributes of an Emissions Model for Policy Making

For an emissions model to assess trade-offs between different emissions as well as the effects of potential future combustor designs, the model should have three features. The emissions model should represent the physical relationships between operating conditions, simplified combustor design parameters, and pollutant emissions in a consistent way. The model should have as inputs, high-level design parameters and operating conditions that would be convienient for an expert to use in projecting future technology. For example, overall fuel-air ratio and inlet pressures and temperatures are more appropriate than detailed specifications of cooling flow geometry and recirculation zone patterns. The model should be general, meaning one modeling methodology can be applied to estimate broad trends in combustor designs across engine manufacturers.

1.3 Current Emissions Prediction Strategies and Techniques

There are currently several techniques used in practice to predict the emissions of aircraft gas turbine combustors. These techniques fall into four general catagories, empirical models, semiempirical models, simplified physics-based models, and high-fidelity simulations. Each method has its strengths and weaknesses and each will be discussed in turn.

1.3.1 Empirical Models

Empirical models tend to be the simplest of the four model types and the least computationally intensive. They are defined here as any emissions model which requires empirically determined constants along with any engine specific conditions (P_3, T_3, mass flow-rate, fuel flow-rate, etc). These models are used mainly for NO_x emissions

and are useful for correlating known historical NO_x emissions for a specific combustor. Equations 1.3 and 1.4 are examples of typical empirical NO_x models.

$$\text{EINO}_x = 0.0042 \left(\frac{P_3}{439} \right)^{.37} \exp \left(\frac{T_3 - 1471}{345} \right) T_4, \tag{1.3}$$

where P_3 is the total pressure at the combustor inlet in psia, T_3 is the total temperature at the combustor inlet in ^oR, and T_4 is the total temperature at the combustor exit in ^oR [11].

$$\text{EINO}_x = 0.068 P_3^{.5} \exp \left(\frac{T_3 - 459.67}{345} \right) \exp \left(\text{humFact} \times 0.0027114 \right) \tag{1.4}$$

where P_3, T_3, and T_4 are defined as before and humFact is a humidity factor that depends on altitude. At sea level, humFact = 0.0063 [11]. These two commonly used empirical models for NO_x show that this type of model usually uses only P_3, T_3, and occasionally T_4 as inputs. Relative humidity is incorporated by including a humidity factor, as in equation 1.4, or by using the Boeing method 2 (BM2) approach [12].

The two empirical models shown above are used for single annular combustors (SAC). Within this group of combustors, NO_x models are generated by fitting empirical constants using the certification data of a combustor. In general, an empirical model can be fit to a single annular combustor using

$$\text{EINO}_x = \beta_1 P_3^{.4} \exp \left(\frac{T_3}{\beta_2} \right), \tag{1.5}$$

by fitting the β coefficients using a least squares approach. Using this technique, each combustor within a given design family will have its own empirical NO_x model that will predict the NO_x emission index for that combustor. The prediction will generally be very good within the range of data used to generate the empirical constants. Different families of combustors have different general forms for empirical NO_x models. Equations 1.6 and 1.7 are empirical NO_x models for dual annular combustors and

lean-premix-prevaporize (LPP) combustors respectively. Both are from [11].

$$\mathrm{EINO}_x = 3.9 P_3^{.37} \exp\left(\frac{T_3 - 459.67}{349.90}\right) \times \exp(\mathrm{humFact} \times 0.002114) \times \mathrm{FAR/delphi} \quad (1.6)$$

where P_3, T_3, and humFact are defined as before and FAR is the fuel-air ratio of the combustor and delphi is a variable that modifies the FAR for different cooling flow regimes. This model is more complex than the simple model for the SAC and may be better described as a semiempirical model. The LPP model is

$$\mathrm{EINO}_x = 0.0000758(P_3 \times 6.8948)^{0.75} \sqrt{\frac{0.0075 T_3}{T_4}} \quad (1.7)$$

where P_3, T_3, and T_4 are all defined as before. There are similar models for rich-quench-lean (RQL) combustors, staged-dual annular combustors, double dome combustors and others. In all cases there is a general form of the empirical model and coefficients are fit on an individual basis for specific combustors.

For situations where the combustor of an engine is fixed and certification data are available, empirical models are easy to generate and are generally regarded as more accurate when applied to engines for which they were derived but not for other engines. Inputs to these models are usually based on P_3 and T_3, which are easily estimated using performance specifications quoted by manufacturers and thus proprietary data is unnecessary. The weaknesses of these types of models are that they are not as accurate when used more generally and that they are useful for predicting emissions only within the bounds of the historical databases on which they are generated. When an empirical model is used for a large variety of combustors within a single family using only a single set of empirical constants, the correlation with any particular combustor tends to be poor. This makes it difficult to use empirical modeling techniques unless an empirical model is generated for every combustor that is to be studied. Since empirical models are generated from fitting a certain number of constants using historical certification data, they cannot be expected to perform as well when the combustor undergoes a design change.

Currently, empirical models for NO_x are used in most large scale engine per-

formance tools (NPSS, NEPP). Each combustor will usually have its own empirical model and the models are not typically used for analyzing the effects of design changes. Another weakness of empirical models is that they do not exist for prediction of CO emissions. This makes it impossible to capture consistent trades between NO_x and CO with empirical modeling techniques, which makes empirical models inadequate for use in a policy-making emissions model.

1.3.2 Semiempirical Models

Semiempirical models consist of equations that contain empirically determined constants, cycle parameters, and experimentally gathered data on residence times, characteristic kinetic times, and other parameters like primary zone temperature. These methods are capable of modeling CO emissions as well as NO_x emissions with separate correlations, which may nor may not be consistent with one another. Equation 1.8 is an example of a semiempirical model for carbon monoxide,

$$\text{EICO} = 35 \times \tau_{CO}/\tau_{sl,CO}, \tag{1.8}$$

where τ_{CO} is a characteristic kinetic time based on a reaction rate constant, and $\tau_{sl,CO}$ is a characteristic quenching time, based on a measured quench length where the overall equivalence ratio of the combustor drops below a certain value, causing the temperature to drop below a critical value that hinders CO oxidation to CO_2 [13]. Equation 1.9 is an example of a semiempirical model for NO_x prediction.

$$\text{EINO}_x = \frac{AV_c P^{1.2} exp(0.009T_{pz})}{\dot{m}_A T_{pz}(\Delta P/P)^{0.5}}, \tag{1.9}$$

where A is a constant, V_c is the combustor primary zone volume, P is pressure, T_{pz} is the primary zone temperature, $\dot{m}_A$ is the primary zone air flow rate, and ΔP is the liner pressure drop [14]. Generally empirical models for NO_x emissions are used in favor of semiempirical models by industry and in tools like NEPP and NPSS.

A weakness of the semiempirical modeling approach is that the outputs, EICO

and $EINO_x$, are very sensitive to the inputs and the inputs are very difficult to obtain, particularly in the case of EICO. Since the relations for different emissions are not related to one another in any way, which could lead to inconsistent predictions of NO_x and CO, and since the models frequently require experiment or expert knowledge of a particular combustor for use, these types of models do not meet the requirements for use in a policy making tool. These models also have limited use for predicting the effects of combustor design changes on emissions because the effects of a design change on the model inputs would likely not be known unless the design change has already been tested physically.

1.3.3 Simplified Physics-Based Models

Simplified physics-based models consist of reduced-order physics and chemistry in ideal reactors aimed at using physical parameters to get useful results at a fraction of the computational burden of a more detailed simulation. These types of models are not widely used for emissions prediction. A weakness of using a simplified physics-based model is that it is possible to get accurate estimates of emissions with a model that is not accurately capturing the physics and chemistry of the combustion process. For example, if a physics-based model does not incorporate two phenomena with opposite effects on a particular output, then in cases where the effects cancel out, the physics-based model will provide a good estimate of the output, but in cases where the effects do not cancel out, the physics-based model will not provide a good estimate of the output. This situation, however, is difficult to account for with a simplified physics-based model. Simplified physics-based models and the ideal reactors of which they consist will be discussed in greater detail in Chapter 2.

1.3.4 High Fidelity Simulations

High fidelity simulations use grids with millions of points, detailed kinetic mechanisms, large eddy simulations (LES), and complex 3D geometries to estimate the products of gas turbine combustion. High-fidelity simulations have been used effec-

tively for some aspects of combustor design, however, they are very computationally intensive, and require detailed knowledge of combustor geometry and operating conditions. Table 1.1 provides data from a NASA Glenn simulation of a GE90 engine to

Component	No. of Iterations	No. of Processors	Wall clock time
Combustor	31000	256	3 hr 53 min

Table 1.1: Full Simulation Time [15]

predict temperature and velocity fields. The table shows that the time and computing power required for this sort of approach is too great for use in a policy making tool. Furthermore, high-fidelity simulations require detailed definitions of the combustor designs, which would not be available for assessing technology trade-offs for potential future combustor designs.

1.3.5 State of the Art for Emissions Trade Analyses

Currently, empirical models are used more than any other type of model because they are general and computationally inexpensive. For trade studies and design change analyses however, empirical models are less useful. Semiempirical models exist to some extent on an individual combustor basis for both NO_x and CO, but the inputs to these models are typically not available when considering the impacts of alternative emissions policies on future engine and combustor configurations. Semiempirical models also would have limited capability for studying the effects of design changes that have not yet been measured. Physics-based models have been shown to have some potential for capturing the interdependencies of emissions as well as combustor performance on a very specific basis. Most of the work done with these models has focused on creating a model to predict the emissions of a single combustor and has not been extended in a general way. Full simulations require detailed definitions of the geometry and operating conditions and are computationally prohibitive.

1.4 A Physics-Based Emissions Model

Given that the physics-based model has the most potential for a general emissions model for a policy tool, a simplified physics-based model was selected for further study to determine whether or not a model of that nature could be developed to meet the three requirements for a policy-making tool referred to in Section 1.2.

1.4.1 Objective

The objective of this research is thus to create a physics-based model for estimating emissions of potential future gas turbine combustors within quantified uncertainty bounds. The method should be capable of predicting various tradeoffs associated with typical changes in the design of a combustor. The emissions model is being designed for use as a component of a policy-making tool, and as such, higher levels of uncertainty are acceptable than would be the case if the model was for use in the design of a combustor.

1.4.2 Emissions Model Success Criteria

The success of the emissions model developed in this thesis is measured by how well the three attributes that make a model suitable for use in a policy making tool are incorporated. The physical relationships among operating conditions, simplified combustor design parameters, and pollutant emissions are assessed by comparing the response of the model emissions outputs to different operating conditions and design parameters to the response that would be expected from theory or the response that is apparent in certification data. A successful model should predict trends that are supported by theory and data. The high-level design parameters and operating conditions that would be convienient for an expert to use in projecting future technology should be built into the model as inputs. How well the model predicts broad trends in the emission levels from different combustor designs is determined by how well the model performs relative to an empirical model for NO_x, and whether or not the model predictions are within the uncertainty in the certification data for CO. The goal is to

produce estimates of the trends in emissions of NOx and CO at a level of accuracy that is valuable in a policy-making setting. In particular, it is desired first that the correct sign be predicted for changes in emissions with design and operating parameters. If this level of performance is met, an additional goal is to predict changes in emissions with changes in design and operating conditions with an accuracy that approaches that of the uncertainty and variability of measurements of emissions indices for the active fleet (e.g. about 16% for NO_x and 23% for CO). Detailed data from five industry combustors were used in the assessment of the model.

1.5 Thesis Outline

Chapter 2 discusses the development of the physics-based emissions models used in the study. Chapter 3 focuses on how primary zone unmixedness is set in the model. Chapter 4 compares the response of the model emissions outputs to changing operating conditions and combustor design parameters. Chapter 5 presents a comparison of the emissions levels predicted by the model to the ICAO certification data and an empirical model for five different engines. The model's ability to predict the effects of a design change is also assessed in Chapter 5. Chapter 6 contains general conclusions about the work as well as a discussion of future work that should be done.

Chapter 2

Developing a Physics-Based Emissions Model

This chapter discusses the developement of a physics-based emissions model for single annular aircraft gas turbine combustors. The functional requirements of the model are discussed followed by the inputs and outputs of the model. Fundamentals of combustion are then reviewed to introduce the governing equations followed by a discussion of ideal reactors. The use of ideal reactors to model each zone of a gas turbine combustor is then discussed.

2.1 Functional Requirements

The physics-based emissions model should have as inputs, high-level design parameters and operating conditions that would be convienient for an expert to use in projecting future technology. The emissions model should also represent the physical relationships among operating conditions, combustor design parameters, and pollutant emissions in a consistent way. The model must also produce estimates of the trends in emissions of NO_x and CO at a level of accuracy that is valuable in a policy-making setting. In particular, it is desired first that the correct sign be predicted for changes in emissions with design and operating parameters. If this level of performance is met, an additional goal is to predict changes in emissions with changes in

design and operating condtions with an accuracy that approaches that of the uncertainty and variability of measurements of emissions indices for the active fleet (e.g. about 16% for NO_x and 23% for CO).

2.2 Model Input/Output

The inputs to the physics-based emissions model are the combustor inlet temperature and pressure, the mass flow rate into the combustor, the fuel flow rate, the mass flow splits, the combustor zone volumes, and the primary zone unmixedness. The inputs are all useful and convienient for expert use and contain the physical relationships between operating conditions and combustor design parameters.

The chemical kinetics taking place in the combustion process are modeled with the Gas Research Institute mechanism (GRImech) version 3.0 for propane [16]. Using GRImech v3.0 ensures that the physical relationships between gaseous pollutant emissions and combustor design parameters and operating conditions are accounted for in a consistent manner.

The outputs from the model are the emissions indices of NO_x ($EINO_x$) and CO (EICO).

2.3 Combustion Fundamentals

Combustion in a gas turbine engine consists of the rapid oxidation of a fuel, which generates heat. For gas turbine combustion, the oxidizer is typically air and the fuel may be liquid or gaseous [14]. The combustion of a fuel-air mixture in an aircraft engine is a complex, unsteady, turbulent process governed by a set of non-linear partial differential equations.

2.4 Governing Equations

The governing equations are the conservation of mass, species, momentum, and energy for a reacting flow. The most general form of mass conservation for a fixed point in a flow may be written as

$$\frac{\partial \rho}{\partial t} + \nabla \cdot (\rho \boldsymbol{u}) = 0, \tag{2.1}$$

where ρ is density and $\boldsymbol{u}$ is velocity. The general form of species conservation for a reacting flow may be written as

$$\frac{\partial (\rho Y_i)}{\partial t} + \nabla \cdot \dot{m}_i'' = \dot{m}_i''' \text{ for i = 1,2,...,N}, \tag{2.2}$$

where Y_i is the mass fraction of species i, $\dot{m}_i''$ is the mass flux of species i, and $\dot{m}_i'''$ is the net rate of mass production of species i per unit volume. The first term on the left of Equation 2.2 is the rate of increase of mass of species i per unit volume. The second term is the net rate of mass flow of species i out by diffusion and bulk flow per unit volume [17]. The conservation of momentum in general form for a reacting flow may be written as

$$\rho \frac{Du_i}{Dt} = -\frac{\partial p}{\partial x_i} + \rho g_i + \frac{\partial}{\partial x_j}\left[2\mu e_{ij} - \frac{2}{3}\mu(\nabla \cdot \boldsymbol{u})\delta_{ij}\right], \tag{2.3}$$

which is a general form of the Navier-Stokes equation. The compressible form of the conservation of momentum must be used because large changes in density can occur in a reacting flow. The unsteady term must be kept because most flows within a gas turbine combustor are turbulent. In Equation 2.3, $\boldsymbol{u}$ is velocity, p is pressure, g is gravitational acceleration, μ is dynamic viscosity, e_{ij} is the strain rate tensor, $e_{ij} \equiv \frac{1}{2}\left(\frac{\partial u_i}{\partial x_j} + \frac{\partial u_j}{\partial x_i}\right)$, and δ_{ij} is the Kronecker delta. The conservation of energy in one dimension may be written as

$$\sum \dot{m}_i'' \frac{dh_i}{dx} + \frac{d}{dx}\left(-k\frac{dT}{dx}\right) + \dot{m}'' u_x \frac{du_x}{dx} = -\sum h_i \dot{m}_i''', \tag{2.4}$$

where h_i is the specific enthalpy of species i, k is the thermal conductivity and u_x is the velocity in the x direction.

The simultaneous solution of these four coupled, non-linear, partial differential equations, (with an appropriate model for turbulence and the kinetic relations for the chemical species), could in theory be solved to provide estimates of species concentrations. Since a detailed geometry definition is required to solve such a problem, the governing equations are too general to meet the objectives of a physics-based emissions model for a policy making tool. To create a physics-based model of gas turbine combustion that does not require detailed geometric specifications, several assumptions that reduce the level of complexity of the governing equations must be made.

2.5 Reducing the Governing Equations

The full set of governing equations includes several aspects of reacting flows that may be neglected if higher levels of uncertainty in the emissions estimates are acceptable. Ideal reactors such as perfectly stirred reactors and plug flow reactors make a number of assumptions that significantly reduce the complexity of the combustion process while still providing useful information.

2.5.1 The Perfectly Stirred Reactor

The perfectly stirred reactor (PSR) is an ideal reactor that neglects mixing phenomena in a reaction. Combustion processes are characterized by the characteristic times certain processes take. In a system where either the mixing rates are high or the chemical reaction rates are slow, the chemical kinetics constrain the burning rates in the mixture. The situation may be characterized by a Damkohler number, Da. The Damkohler number is defined as

$$Da \equiv \frac{\tau_{flow}}{\tau_{chem}}, \tag{2.5}$$

where τ_{flow} is a characteristic mixing time and τ_{chem} is a characteristic chemical time [18]. In situations where $Da \ll 1$, the burning rate is almost completely dependent on the chemical kinetics of the mixture. When this is the case, calculations that ignore mixing phenomena, like convection and diffusion, and focus only on the kinetic modeling may be used.

The perfectly stirred reactor (PSR) assumes that the Damkohler number is essentially zero and thus the mixture is considered perfectly stirred. Mixing has no effect on the system and is not included in the calculations. This assumption allows for a large reduction in the complexity of the governing equations.

Conservation Equations for the PSR

Following Turns [17], the conservation equations for the perfectly stirred reactor may be written as follows. The control volume for the analysis is shown in Figure 2-1. Mass conservation for an arbitrary species i may be written as

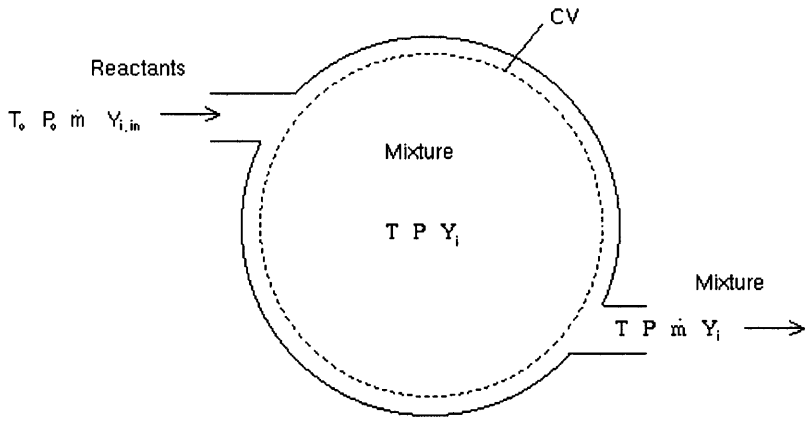

Figure 2-1: Diagram of a Perfectly Stirred Reactor, adapted from [17]

$$0 = \dot{m}_i'''\forall + \dot{m}_{i,in} - \dot{m}_{i,out}, \tag{2.6}$$

where $\dot{m}_i'''\forall$ is the rate of generation or destruction of mass of the i^{th} species, $\forall$ is the volume, $\dot{m}_{i,in}$ is the mass flow of the i^{th} species into the control volume, and $\dot{m}_{i,out}$ is the mass flow of the i^{th} species out of the control volume. The generation or destruction of a species is written as

$$\dot{m}_i''' = \dot{\omega}_i MW_i, \tag{2.7}$$

where $\dot{\omega}_i$ is the net production rate of the i^{th} species in mol/m^{3}s and MW_i is the molecular weight of the i^{th} species in kg/mol. The mass flow of the i^{th} species into the control volume is the mass flow in multiplied by the initial mass fraction of the species, or

$$\dot{m}_{i,in} = \dot{m}Y_{i,in} \tag{2.8}$$

and similarly, the mass flow out of the control volume is

$$\dot{m}_i = \dot{m}Y_i. \tag{2.9}$$

The mass fraction of a species is the individual mass of the i^{th} species in the mixture divided by the total mass of the mixture.

The conservation of energy for the perfectly stirred reactor may be written as

$$\dot{Q} = \dot{m}(h_{out} - h_{in}). \tag{2.10}$$

In terms of the individual species this is

$$\dot{Q} = \left(\sum_{i=1}^{N} Y_{i,out} h_i(T) - \sum_{i=1}^{N} Y_{i,in} h_i(T_{in}) \right), \tag{2.11}$$

where h_i is the specific enthalpy of the i^{th} species, which is written as

$$h_i(T) = h_{f,i}^o + \int_{T_{ref}}^{T} c_{p,i}(T) dT. \tag{2.12}$$

The term $h^o_{f,i}$ is the enthalpy of formation of the i^{th} species and $c_{p_i}(T)$ is the specific heat of the i^{th} species, which is a function of the temperature of the mixture.

The Mathematical Simplicity of the Perfectly Stirred Reactor

Since there is no dependence on flow parameters there is no conservation of momentum equation for the perfectly stirred reactor. Also, because the reactor is operating at steady-state, there is no time dependence in the conservation equations. As a result the perfectly stirred reactor is described fully by a set of coupled nonlinear algebraic equations instead of a system of non-linear partial differential equations. The result is that problems dealing with perfectly stirred reactor models may be solved using a Newton-Raphson approach.

2.5.2 PLUG Flow Reactor

A plug flow reactor is an ideal reactor that assumes steady, one-dimensional, inviscid flow with ideal gas behaviour. The assumptions imply that there is no mixing in the axial direction. The control volume for the conservation equations that follow refer to Figure 2-2. The conservation equations for a plug flow reactor may be written as

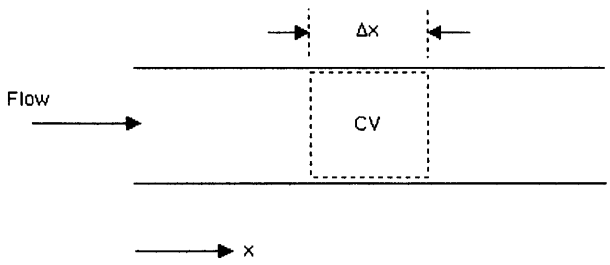

Figure 2-2: Diagram of a Plug Flow Reactor, adapted from [17]

Conservation of Mass:

$$\frac{d(\rho u_x A)}{dx} = 0, \tag{2.13}$$

Conservation of Momentum:

$$\frac{dp}{dx} + \rho u_x \frac{du_x}{dx} = 0, \tag{2.14}$$

Conservation of Species:

$$\frac{dY_i}{dx} - \frac{\dot{\omega}_i MW_i}{\rho u_x} = 0, \tag{2.15}$$

Conservation of Energy:

$$\frac{dT}{dx} = \frac{u_x^2}{\rho c_p}\frac{d\rho}{dx} + \frac{u_x^2}{c_p}\left(\frac{1}{A}\frac{dA}{dx}\right) - \frac{1}{u_x \rho c_p}\sum_{i=1}^{n} h_i \dot{\omega}_i MW_i, \tag{2.16}$$

The Mathematical Simplicity of the Plug Flow Reactor

The assumptions of the plug flow reactor reduce the coupled, non-linear, three-dimensional governing equations of combustion to a set of coupled ordinary differential equations, for which many efficient solution methods exist.

2.6 Modeling a Gas Turbine Combustor with Ideal Reactors

A gas turbine combustor typically consists of a primary zone, an intermediate zone, and a dilution zone. To represent the physical relationships among operating conditions, pollutant emissions, and combustor design parameters like zone volumes, the emissions model should be developed to capture the physical layout of a combustor.

2.6.1 The Role of the Primary Zone

The primary zone of a gas turbine combustor is designed to anchor the flame and achieve nearly complete combustion of the fuel. To do this, the primary zone must provide sufficient residence time for the fuel-air mixture, as well as high temperatures and high turbulence for rapid mixing of the fuel and air. For these reasons primary zones of typical combustors have large recirculation regions of flow, high temperatures,

and high levels of turbulence.

2.6.2 Modeling the Primary Zone

Regions of strong turbulence in a combustion process tend to have short characteristic mixing times relative to the kinetic times. The result is that these regions have low Damkohler numbers. This suggests that the primary zone could be modeled using a PSR, which assumes instantaneous mixing with a Damkohler number of zero. Figure 2-3 shows the effects of increasing levels of turbulence intensity on Damkohler number and how the combustion should be modeled. Turbulence intensity, V_t/S_u, which is the ratio of characteristic turbulence velocity to the laminar flame speed, is plotted on the vertical axis, and a length scale ratio, l_t/Δ_F, which is the ratio of the turbulence length scale to the flame thickness, is plotted on the horizontal axis. The Damkohler number is related to these scales by

$$\frac{V_t}{S_u} = \frac{1}{Da}\frac{l_t}{\Delta_F}. \tag{2.17}$$

Both the equation and the figure show that as turbulence intensity increases, the Damkohler number decreases. The figure shows that as the Damkohler number decreases, the combustion process becomes more and more suitable for modeling with a stirred reactor. With the high level of turbulence expected in the primary zone for most engine power settings, the PSR has the potential for being an appropriate model.

2.6.3 Primary Zone Emissions Considerations

Using only a single PSR to model the primary zone of a combustor implies that the entire fuel-air mixture is perfectly mixed and remains so throughout the zone. In a real combustor, however, fuel and air are injected separately, and this ideal situation cannot be expected to prevail. This means that the Damkohler number is not likely to be close enough to zero for a single PSR to be an adequate model for emissions of NO_x and CO, which are highly sensitive to the local fuel-air ratio in the combustor.

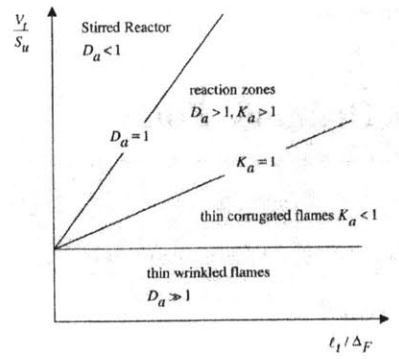

Figure 2-3: The Effect of Turbulence on Damkohler Number [18]

The activation energy of NO_x is strongly dependent on temperature and thus on local equivalence ratio. For CO, if the local equivalence ratio is greater than unity, large amounts of CO will be formed due to lower oxygen concentration for completing the reaction to CO_2. For equivalence ratios close to unity, large amounts of CO will form because of CO_2 dissociation. For very low equivalence ratios ($\phi < 0.6$), the mixture strength cannot support complete combustion and CO is formed in great quantities farther down the combustor. According to Lefebvre [14], only for equivalence ratios of about 0.7-0.9 will low levels of CO be formed. Therefore, if CO emissions are to be properly calculated, any deviation from a perfect mixture in the primary zone must be accounted for to ensure that local equivalence ratios are correct. Due to these considerations, the model of the primary zone should include some mechanism for incorporating varying levels of unmixedness.

Modeling Unmixedness in the Primary Zone

A typical approach for capturing the unmixedness in a combustor is to assume that the mixture can be approximated by a normal distribution about some mean equivalence ratio [24]. The distribution is then defined by an unmixedness parameter, s, where

$$s = \frac{\sigma_\phi}{\mu_\phi}, \tag{2.18}$$

and σ_ϕ is the standard deviation of the distribution and μ_ϕ is the mean equivalence ratio. This technique has been used numerous times [19]. Figure 2-4 shows how the

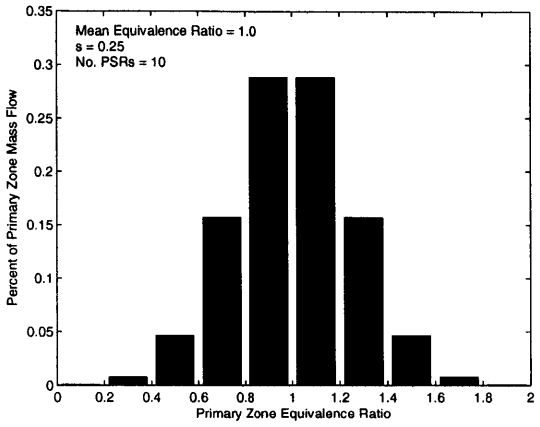

Figure 2-4: Normal Distribution of Equivalence Ratio in the Primary Zone PSRs

equivalence ratios and mass flow percentages through a set of 10 PSRs are set with an unmixedness value of $s = 0.25$ and a mean equivalence ratio of $\phi_p = 1$. The equivalence ratios are determined using Equation 2.18 and the mass flow percentages are calculated from the cumulative distribution function and are shown on the vertical axis.

To determine how many PSRs should be used for the distribution, a variable number of PSRs were run to represent the primary zone of a combustor, followed by a PSR to represent the intermediate zone and a plug flow reactor to represent the diluton zone. The inputs were taken from an industry gas turbine combustor. The emissions output from the different cases were plotted to determine when adding more PSRs no longer had a significant impact on the emissions indices. The outputs of interest are the emissions indices of NO_x and CO. The percentage change in emissions indices for NO_x and CO were calculated as

$$\%\Delta_{\mathrm{EINO}_x}(i+1) = \frac{\mathrm{EINO}_x(i+1) - \mathrm{EINO}_x(i)}{\mathrm{EINO}_x(i)} \tag{2.19}$$

$$\%\Delta_{\mathrm{EICO}}(i+1) = \frac{\mathrm{EICO}(i+1) - \mathrm{EICO}(i)}{\mathrm{EICO}(i)} \tag{2.20}$$

where the values i and $i+1$ refer to the number of PSRs in the model and $i = 1, ..., 39$. The number of PSRs was considered adequate when the percentage change with each additional reactor in $EINO_x$ fell below 5% and the percentage change in EICO fell below 15% for all four ICAO engine power settings. The reason for this was that the 90% confidence interval for new, uninstalled engines picked out of a fleet is $\pm 16\%$ for $EINO_x$ and $\pm 23\%$ for EICO [20]. Since the desired accuracy of the model is to be within the uncertainty in the data, the addition of more PSRs beyond the uncertainty in the data has no impact on whether or not the objectives of the model will be met. Stricter criteria than the uncertainty in the data were used because the values for the uncertainty in the NO_x and CO emissions data are considered conservative. The results of the analysis are shown in Figure 2-5. The data was collected with an

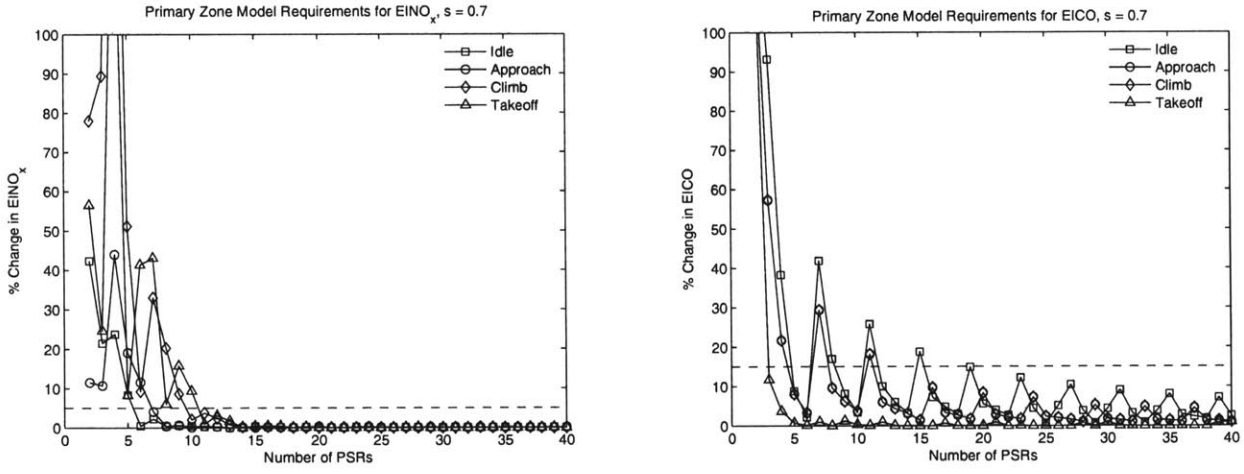

(a) $EINO_x$ (b) EICO

Figure 2-5: Determining the Primary Zone Model

unmixedness level of $s = 0.7$, which is the highest value of primary zone unmixedness that is expected to occur [19]. Higher levels of unmixedness require more reactors to appropriately reflect the normal distribution, which is why the unmixedness level was chosen at the highest level. The plots show that for $EINO_x$ to be modeled adequately with a normal distribution, there must be at least eleven PSRs in the primary zone. For EICO to be modeled adequately, there must be at least sixteen PSRs in the

primary zone. Therefore, to ensure that the normal distributions are being modeled well enough, the primary zone model consists of sixteen parallel PSRs. Figure 2-6 is a diagram of the primary zone model.

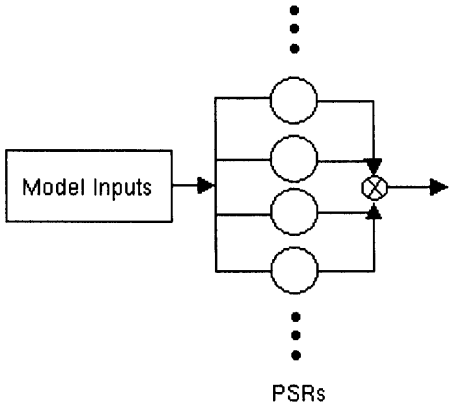

Figure 2-6: Diagram of the Primary Zone Model

2.6.4 Assumptions and Limitations of the Primary Zone Model

The main assumption of the primary zone model is that local mixing is instantaneous relative to local burning. This results in a premixed flame in each of the primary zone PSRs. Unfortunately, in most liquid fueled gas turbine engines, the combustion process is governed by diffusion flame phenomena, meaning that the burning occurs at stoichiometric fuel-air ratios. Equivalence ratios of unity lead to high flame temperatures and thus high NO_x production, implying that a model consisting only of premixed flames may not calculate the emissions index of NO_x accurately in some cases, particularly in older combustors where attempts at some level of premixing were not made.

Another assumption of the primary zone model is that each individual reactor is essentially zero-dimensional and everything occurs at once. In an actual combustor primary zone, cooling air is gradually added and the fuel and air gradually mix. This assumption could have a significant effect on CO emissions since a mechanism for quenching reactions occurring near the combustor walls is not possible with this

model.

2.6.5 The Role of the Intermediate Zone

The intermediate zone of a combustor is designed to recover dissociation losses, burn poorly mixed fuel-rich pockets at low altitude and serve as an extension of the primary zone at high altitude. At low altitude, the high temperature conditions of the primary zone lead to the dissociation of CO_2 to CO. If the reaction is then quenched the CO concentration will essentially be frozen, leading to high CO output. The intermediate zone's role is then to slowly add dilution and cooling air while maintaining a high enough temperature to complete combustion. Pockets of fuel-rich mixture may also exist leaving the primary zone which must be burned in the intermediate zone otherwise there will be a penalty in combustion efficiency. At high altitude combustion is usually not complete at the exit of the primary zone because the fuel-air concentration is lower, due to lower pressure, which leads to reduced reaction rates. In this case the combustion process continues in the intermediate zone. These requirements lead to a trade off in the intermediate zone between zone length, which determines the residence time, and combustion efficiency.

2.6.6 Modeling the Intermediate Zone

To determine how to best model the intermediate zone, six candidate intermediate zone reactor setups were studied and the output of each model was compared to emissions data. Six candidate reactor setups were studied because it was unclear how to best model the intermediate zone. The six candidate reactor setups were a single plug flow reactor, a single PSR, a set of parallel plug flow reactors, a set of parallel PSRs, a bulk plug flow reactor with a wall plug flow reactor, and a bulk plug flow reactor with a wall PSR. The single plug flow reactor was tested because it would be an appropriate model if the mixing of fuel and air in the primary zone, as well as added cooling air and dilution air prior to the intermediate zone, is complete. For this situation the plug flow reactor could be used to simulate a one-dimensional

reacting flow. A single PSR was tested because it would be an appropriate model if recirculation due to the addition of downstream dilution air and cooling air is present in the intermediate zone. Parallel plug flow reactors and parallel PSRs were tested because they would be a more appropriate model for the intermediate zone if the effects of a non-uniform mixture, due to the addition of cooling air and dilution air along the walls of the combustor, are significant in terms of emissions output. Modeling the bulk flow with a single plug flow reactor and the flow near the walls of the combustor intermediate zone, where CO is not likely to oxidize to CO_2 due to the lower temperatures, with a PSR or a plug flow reactor was tested because of the possibility that most of the CO formed during combustion is due to quenching near the walls of the combustor.

Testing each candidate intermediate zone model revealed that the single plug flow reactor provided the best results. The single PSR reactor significantly overestimated CO at low power. The set of parallel PSRs and plug reactors yielded poor predictions of both NO_x and CO at all conditions and the wall reactor setups were too sensitive to flow split information in the intermediate zone to be used in a general model. The single plug flow reactor provided the best CO and NO_x estimates and was selected for the intermediate zone model. Figure 2-7 is a diagram of the intermediate zone

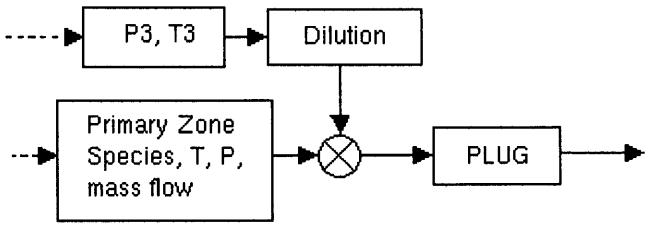

Figure 2-7: Diagram of the Intermediate Zone Model

model.

2.6.7 Intermediate Zone Emissions Considerations

The formation of NO in a gas turbine combustor only proceeds at a significant rate at temperatures above around 1800K [14]. Since these high temperatures are expected to occur mainly in the primary zone, the effect of the intermediate zone model on NO_x emissions is negligible as seen in Chapter 4. Since the intermediate zone is designed to complete the combustion of the mixture leaving the primary zone, the intermediate zone oxidizes most of the CO to CO_2.

2.6.8 Assumptions and Limitations of the Intermediate Zone Models

The main assumption of the intermediate zone model is the instantaneous addition of cooling air and dilution air. This is not expected to impact NO_x output significantly, but it may have an effect on CO emissions. Gradual air addition would allow for higher zone temperatures, which would lead to more CO oxidation to CO_2. The assumption may therefore, lead to overestimates of CO emissions.

2.6.9 The Role of the Dilution Zone

The dilution zone of a gas turbine combustor is designed to bring the gas to an acceptable mean temperature and to improve the pattern factor prior to the turbine inlet. At most power conditions combustion has essentially been completed and the emissions of NO_x and CO are not changed. At low power it is possible that further CO oxidation may take place but the addition of dilution air and cooling air will usually reduce the temperature to the point where these reactions are no longer taking place.

2.6.10 Modeling the Dilution Zone

The flow in the dilution zone is essentially one-dimensionally moving towards the turbine and should be modeled reasonably well with plug flow reactors. The model for the dilution zone is thus two serial plug flow reactors, one for the initial addition

of dilution air, which could potentially have an impact on CO emissions, and another for the addition of pattern factor cooling air. Figure 2-8 is a diagram of the dilution

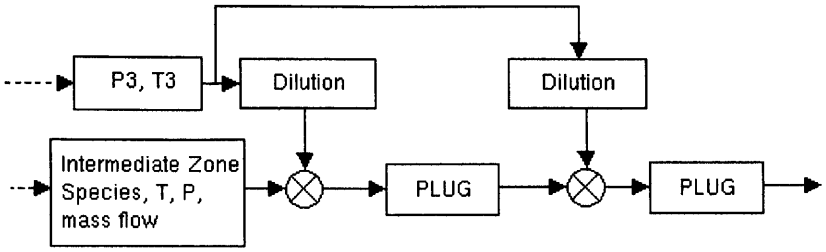

Figure 2-8: Diagram of the Dilution Zone Model

zone model.

2.6.11 Modeling the Injection of Dilution/Cooling Air

Gas turbine combustors usually have two main forms of air addition that serve two different purposes. Dilution air is usually injected in two major locations and its purpose is to bring the gas temperature to the point where CO is still oxidizing to CO_2, but NO_x is no longer being formed in major quantities, and also to reduce the mean gas temperature prior to turbine entry. Cooling air is injected along both the inner and outer diameter of the combustor liner and its purpose is to protect the liner material from the hot temperatures of the reacting bulk flow. Where and how much air is injected into the combustor is defined by flow splits and geometry, which define where the flow is introduced into the combustor and what percentage of the total air mass flow rate comes through each cooling slot and dilution hole. Figure 2-9 is an example of a set of flow splits for a given combustor geometry. The letters in the figure would be different percentages of mass flow rate entering at each location. The difficulty with the flow split information is determining how to map the flow split inputs from the physical domain to the model domain. The model consists of air addition only at two main dilution points and a final cooling air addition point. The challenge is thus to determine when the air flow from each of the physical injection

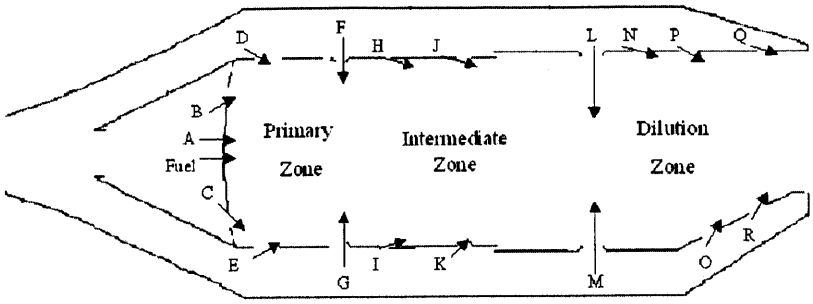

Figure 2-9: Typical Combustor Flow Splits

points mixes in with the bulk flow. Several possibilities for this were tested and it was found that assuming the cooling air mixes into the bulk flow when it encounters a dilution jet provides the best results. This means that in the model, the flow entering at location D is combined with the flow from location F because the injection at D is cooling air that has encountered a main dilution injection at location F. The assumption allows for simple transitions from combustor to combustor even though the geometries and flow splits are usually unique to individual combustors.

2.6.12 Assumptions and Limitations of Injection Mapping

A major assumption of the modeling of air addition into the combustor is that it is not necessary to exactly match the geometry and flow split inputs of the physical combustor in the model domain to calculate emissions of NO_x and CO. However, since CO emissions can in some cases be the result of CO from the primary zone becoming entrained into the cool air along the liner and then failing to oxidize because of the lower temperatures, the air addition model may lead to erroneous CO predictions in some cases. This is because the model does not permit gradual addition of cooling air along the walls of the combustor where the CO from the primary zone could become entrained.

2.6.13 Model Implementation

The ideal reactors that make up the physics-based emissions model are run using Chemkin version 4.0. The inputs, reactor linking, air addition, and output calculations are all done with Matlab.

2.6.14 The Physics-Based Emissions Model

Figure 2-10 is a diagram of the simple physics-based emissions model that was created. The primary zone is modeled as a network of 16 parallel PSRs, the intermediate zone is modeled as an injection of air followed by a plug flow reactor, and the dilution zone is modeled as an injection of air followed by a plug flow reactor, followed by another injection of air and another plug flow reactor.

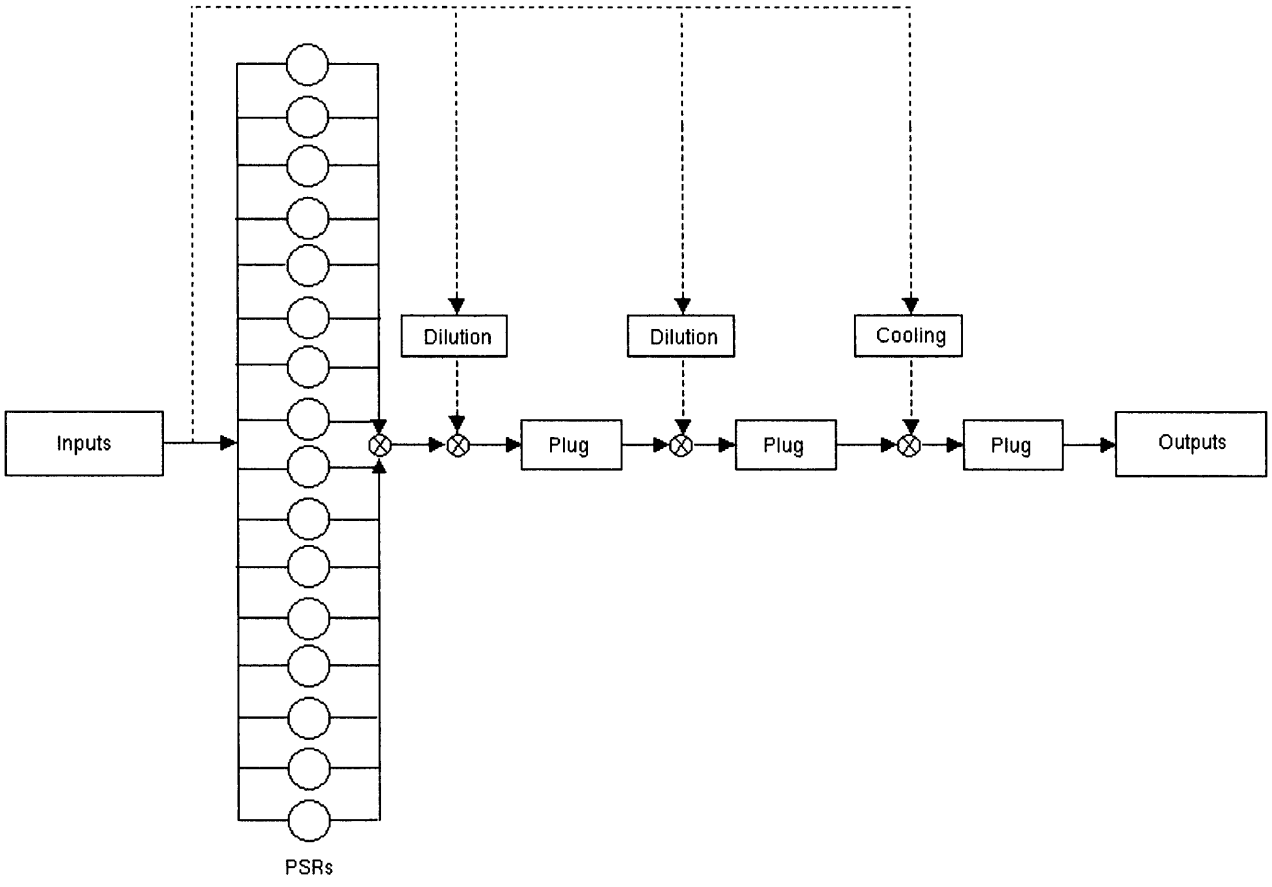

Figure 2-10: Diagram of the Physics-Based Emissions Model

Chapter 3

Setting the Unmixedness Parameter

All of the inputs to the physics-based emissions model are measured physical quantities with the exception of primary zone unmixedness. The primary zone unmixedness is a physical parameter, but it is not typically measured by industry. The physical nature of this parameter stems from the level of mixing between fuel and air that occurs in the primary zone of the combustor. There are several different options for how the unmixedness parameter can be set. Among these are setting the unmixedness level as a constant value at all engine power settings, setting the unmixedness level as a function of primary zone equivalence ratio and using the relation generally across all engines, and setting the unmixedness level as a function of primary zone equivalence ratio for each individual baseline combustor. Setting a single value of unmixedness across all engine power settings assumes that the unmixedness is only a function of primary zone geometry. Setting the unmixedness using a general relationship between unmixedness and primary zone equivalence ratio implies that the unmixedness is only a function of the fuel-air ratio and is independent of geometry. Setting the unmixedness as a function of primary zone equivalence ratio for each baseline combustor assumes that the unmixedness could be a function of both geometry and fuel-air ratio. Testing each method revealed that the unmixedness should be set as a function of primary zone equivalence ratio for each individual baseline combustor

because the unmixedness is a function of both fuel-air ratio and combustor primary zone geometry.

3.1 Industry Data

Industry data were used to study the effects of the unmixedness parameter and how it is set. The data came from five different combustors on five different gas turbine engines in the same engine line. Table 3.1 gives the relative power of each engine and how the engines are labeled in the study. Engine 1a is the result of a design change

	Engine 1	Engine 1a	Engine 2	Engine 3	Engine 3a
Relative Power	Medium	Medium	Low	High	High

Table 3.1: Relative Power of Each Engine in the Study

on Engine 1 and Engine 3a is the result of a design change on Engine 3.

3.2 Sensitivity to Unmixedness

To determine the impact of the unmixedness parameter on the model output, the sensitivity of NO_x and CO emissions to primary zone unmixedness was studied at each ICAO LTO-cycle point. The unmixedness parameter was varied from 0 to 0.7 at all four power settings for Engine 1a. The results are shown in Figure 3-1. Given that the emissions of NO_x and CO are strong functions of unmixedness, particularly for idle CO, the method of setting unmixedness is crucial to meeting the objective of estimating emissions within the uncertainty in the certification data.

3.2.1 Single Value Optimization

Using a single value for the primary zone unmixedness of a combustor is useful if the unmixedness parameter is set largely by the geometry of the combustor. That is, if the unmixedness parameter is determined almost entirely by the injection methods and the locations of air and fuel injection in the primary zone. If the assumption that

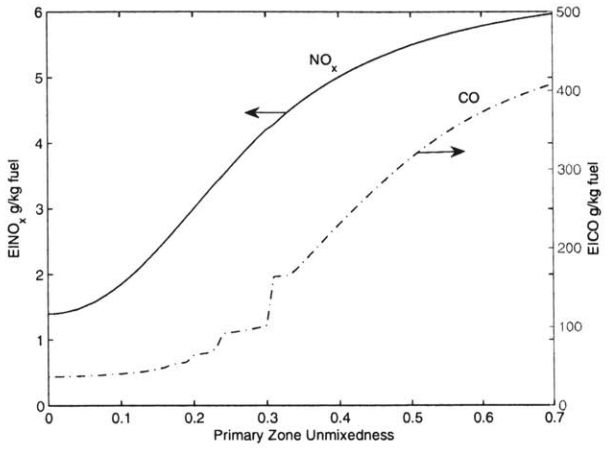

(a) Idle

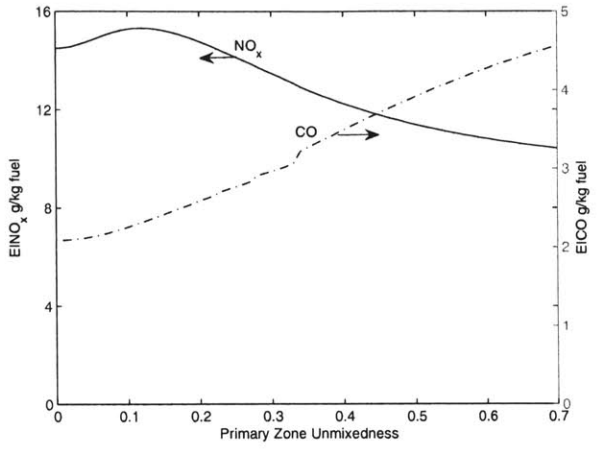

(b) Approach

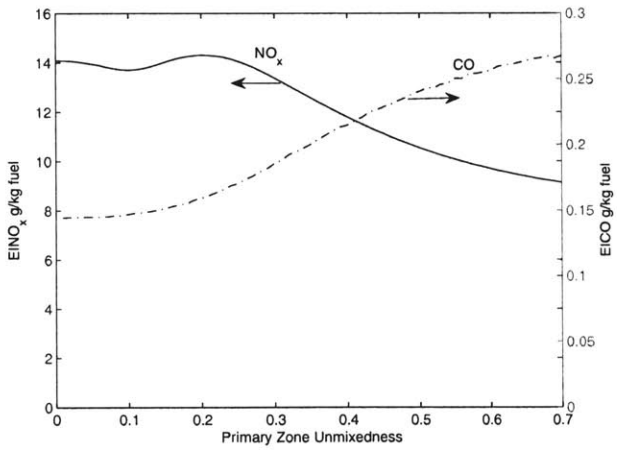

(c) Climb Out

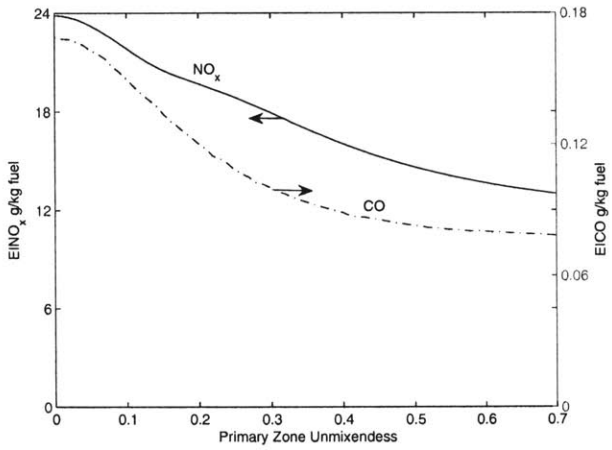

(d) Takeoff

Figure 3-1: Response of Engine 1a Emissions to Varying Unmixedness

the parameter is set largely by geometry is correct, then a single value of unmixedness should work well across different engine settings and combustors with similar geometries.

Setting the unmixedness to a single value is done by optimizing the unmixedness so as to minimize the difference between model and ICAO Dp/Foo for both NO_x and CO. The differences in Dp/Foo for NO_x and CO were calculated using Equations 3.1 and 3.2. The objective function for the optimization is given in Equation 3.3.

$$\Delta\text{Dp/Foo NO}_x = \text{ICAO Dp/Foo NO}_x - \text{Model Dp/Foo NO}_x \tag{3.1}$$

$$\Delta\text{Dp/Foo CO} = \text{ICAO Dp/Foo CO} - \text{Model Dp/Foo CO} \tag{3.2}$$

$$f = \frac{(\Delta\text{Dp/Foo NO}_x)^2 + (\Delta\text{Dp/Foo CO})^2}{\text{ICAO Dp/Foo NO}_x + \text{ICAO Dp/Foo CO}} \tag{3.3}$$

The results of using this method for calculating the unmixedness for the five industry combustors are given in Table 3.2. The combustors used in the analysis are all

	Engine 1	Engine 1a	Engine 2	Engine 3	Engine 3a
Unmixedness	0.30	0.02	0.34	0.19	0.27

Table 3.2: Single Value Optimized Unmixedness

very similar geometrically so the differences between the unmixedness values of each combustor suggest that the parameter should not only be set by geometry.

3.2.2 General Curve Optimization

To set a general curve for the unmixedness parameter, unmixedness was optimized at each ICAO LTO certification point for each engine. Following Sturgess, the unmixedness values were then fit with a polynomial as a function of equivalence ratio [19]. This technique is useful if the unmixedness is not a function of geometry but only a function of primary zone equivalence ratio. The objective function for these

optimizations is shown in Equation 3.4.

$$f_i = \frac{(\text{ICAO EINO}_{xi} - \text{Model EINO}_{xi})^2 + (\text{ICAO EICO}_i - \text{Model EICO}_i)^2}{(\text{ICAO EINO}_{xi} + \text{ICAO EICO}_i)}, \quad (3.4)$$

where the subscript i, refers to the ICAO LTO cycle point (idle, approach, climb out, or takeoff). Figure 3-2 shows the result obtained by Sturgess et al [19]. Figure 3-3 shows the result obtained by using the physics-based model. The square data points in Figure 3-2 are individually optimized unmixedness values for the same three engines used in the analysis of a single value unmixedness optimization as well as Engine 1a and Engine 3a. The figures show there is a relationship between unmixedness and

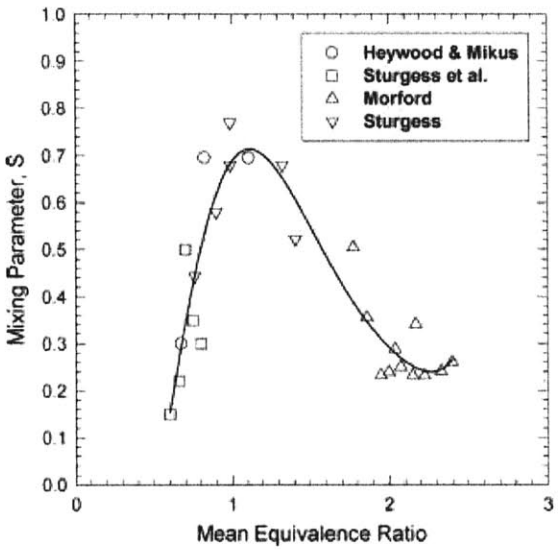

Figure 3-2: Unmixedness versus Primary Zone Equivalence Ratio [19]

primary zone equivalence ratio that should be accounted for. This is expected since combustors are designed to mix fuel and air very well at a design point and will likely not mix it as well at off-design points since the geometry is fixed. The fit for this relationship with a fourth-order polynomial has an R^2 value of 0.74. Figure 3-3 shows that the data point with the lowest value of primary zone equivalence ratio is far from the curve. This point is the optimized unmixedness value for Engine 3a at idle and given the sensitivity of idle CO to unmixedness, idle CO will not be predicted well by the model if this technique of setting primary zone unmixedness is used.

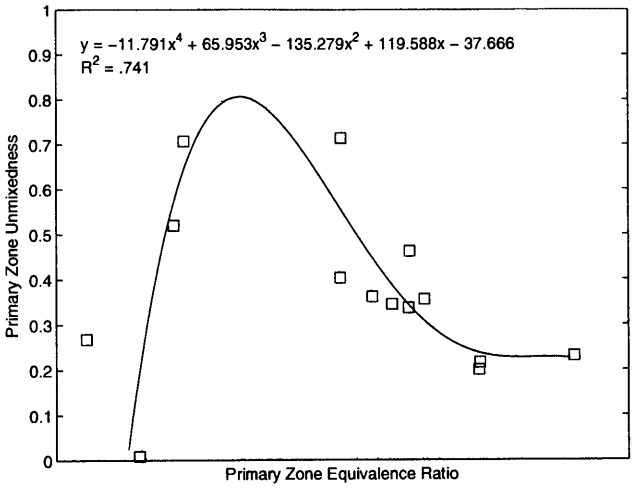

Figure 3-3: Model Unmixedness versus Primary Zone Equivalence Ratio

3.2.3 Individual Curve Optimization

The third option for setting the unmixedness parameter is to set the relationship between primary zone unmixedness and equivalence ratio for each individual baseline engine. The objective of this is to capture the relationship between unmixedness and equivalence ratio while allowing different combustors to have different curves. The curves are developed using the certification data for existing engines and do not require any additional inputs. This allows for the effects of geometry as well as the level of premixing of fuel and air to also be accounted for on an individual engine basis. Once the unmixedness curve for a baseline combustor is set, design changes on that combustor can be studied using the established curve. The optimization technique used to set the unmixedness at each power setting was the same as for the general curve. The result for Engine 1a is shown in Figure 3-4. The curve was fit to the square data points, which are the optimized unmixedness values for Engine 1a at the four ICAO-LTO cycle points.

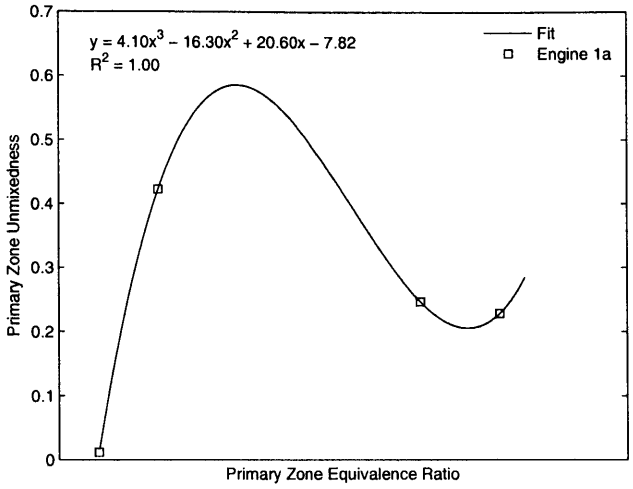

Figure 3-4: Model Unmixedness versus Primary Zone Equivalence Ratio for LTO Cycle

3.3 Evaluating the Different Options

To determine which method of setting the unmixedness is most appropriate, the single point method and the individual curve method were used to set the unmixedness for Engine 1a using the known emissions data for that engine. The unmixedness calculations from Engine 1a were then used on Engine 1 in the same manner that they would be if one were trying to predict the impacts of the design change from Engine 1a to Engine 1. The emissions data for Engine 1 were then used to calculate individually optimized unmixedness values at each engine setting and the results were compared to each method of setting unmixedness.

3.3.1 Single Point Estimate

Using the single point optimization on Engine 1a yields an unmixedness value of $s = 0.02$. To study the effects of the design change from Engine 1a to Engine 1, the unmixedness value calculated for Engine 1a is assumed to be valid for Engine 1 at all power settings. Table 3.3 compares the optimized unmixedness values for Engine 1 using the certification data and the value of unmixedness calculated from Engine 1a.

The comparison shows that the geometry is not the only factor responsible for the

	Idle	Approach	Climb Out	Takeoff
Engine 1 Calculation	0.02	0.02	0.02	0.02
Engine 1 Optimization	0.25	0.70	0.34	0.20

Table 3.3: Comparison of Engine 1 Calculated and Optimized Unmixedness

unmixedness levels in the primary zone of the combustor and that a single value of unmixedness for all engine power settings is not adequate for assessing the effects of design changes.

3.3.2 General Curve Estimate

The general polynomial fit of the relationship between primary zone unmixedness and primary zone equivalence ratio was derived using data from all five engines. To determine how well the curve set the unmixedness for a design change, unmixedness values for Engine 1 were calculated using the curve and compared to the actual optimized unmixedness values for Engine 1 set by the ICAO certification data. The comparison is shown in Table 3.4. The table shows that the general curve produces

	Idle	Approach	Climb Out	Takeoff
Curve Calculation	0.53	0.65	0.34	0.24
Engine 1 Optimization	0.25	0.70	0.34	0.20

Table 3.4: Comparison of Engine 1a Calculated and Optimized Unmixedness

good estimates of unmixedness at all of the ICAO points except idle, where the unmixedness estimate is off of the optimized value by more than 100%.

3.3.3 Individual Curve Estimate

The individual polynomial fit was set using the certification emissions data for Engine 1a. To determine how well the curve set the unmixedness for a design change, unmixedness values of Engine 1 were calculated using the curve and compared to the optimized unmixedness values for Engine 1 set by the ICAO certification data. The comparison for this case is shown in Table 3.5. The best estimate of the unmixedness

	Idle	Approach	Climb Out	Takeoff
Curve Calculation	0.40	0.46	0.38	0.25
Engine 1 Optimization	0.25	0.70	0.34	0.20

Table 3.5: Comparison of Engine 1a Calculated and Optimized Unmixedness

value at idle is obtained using this method. The approach estimate is not as good as the general curve approach estimate, but the sensitivity of the emissions outputs, particularly CO, are much higher at idle, as shown in Figure 3-1.

3.4 Setting Unmixedness

To meet the objectives of the model, the individually derived unmixedness curve method was selected. Since one of the objectives of the model is to estimate the emissions of NO_x and CO within the uncertainty in the certification data, the general curve method, which produces good estimates of unmixedness at approach, climb-out, and takeoff, cannot be used because of the poor estimate of idle unmixedness. The single value method cannot be used because the estimates of unmixedness are poor at all four ICAO certification points. The individually derived unmixedness curve method provides the only means of estimating idle unmixedness in a way that the objective of calculating CO emissions within the uncertainty in the data could be met. For more general applications of the model to future combustors where certification measurements on similar combustors do not exist, it will be necessary to apply the general curve fit method.

3.5 Unmixedness Parameter Issues

The reason the unmixedness is difficult to estimate is likely due to a number of issues that are not accounted for in the model but are compensated for by the unmixedness. The unmixedness parameters exist in the physics-based model to capture the effects of incomplete mixing of the fuel and air injected into the primary zone of a combustor. Unfortunately, the parameter contains more than just a measure of this unmixedness.

It also serves as a correction factor in the model for everything that the model does not capture very well. Issues like the use of a gaseous fuel rather than a liquid fuel, instantaneous mixing of cooling air and dilution, incomplete kinetic modeling, as well as unmixedness are all compensated for by this single parameter. It is not the intention of the model to use unmixedness as a factor for calibrating the model and covering up modeling errors but it is difficult to separate physical unmixedness from everything else that is occuring in the combustor. The issue is exacerbated by the fact that there are no non-proprietary industry data on unmixedness, meaning that the only way to determine an initial level of unmixedness is to set it using certification emissions data.

Given that a more rigorous method of setting the unmixedness level would require a model that deals with the effects of fuel evaporation, gradual air addition, and complete kinetics, which would not meet the objective of creating an emissions model for a policy making tool, the ability to estimate approximately how a design change affects unmixedness, thereby capturing the physical relationship between combustor design parameters like the primary zone geometry and operating conditions like the fuel-air ratio, is considered adequate. Looking at Table 3.6, which shows the optimized values of unmixedness at each condition for Engines 1a and 1, and the calculated unmixedness for Engine 1 using the unmixedness curve derived for Engine 1a, it is clear that at each LTO-cycle point, the effects of the design change from Engine 1a to Engine 1 on unmixedness, with the exception of takeoff are captured correctly. That is, the unmixedness from Engine 1a to Engine 1 increases at idle, increase at approach, and increases at climb out, as they should. At takeoff the unmixedness should have decreased from Engine 1a to Engine 1 but the curve did not predict this correctly. The value of unmixedness at takeoff for each engine however, is within 25% of the optimized value for Engine 1.

	Idle	Approach	Climb Out	Takeoff
Engine 1a Optimization	0.01	0.42	0.24	0.22
Engine 1 Optimization	0.25	0.70	0.34	0.20
Engine 1 Curve Calculation	0.40	0.46	0.38	0.25

Table 3.6: Comparison of Engine 1a Calculated and Optimized Unmixedness

Chapter 4

Assessing the Predictive Capability of the Model

In this chapter, the response of the emissions model to critical inputs is examined and the results are compared to theory. The goal is to establish confidence in the predictive capability of the model.

4.1 NO_x Chemistry

As mentioned previously, NO_x emissions from gas turbine combustors include NO and NO_2. Most of the chemical reactions taking place lead first to NO formation and then, when temperatures are reduced, to the formation of NO_2. After some time in the atmosphere essentially all of the NO produced in the combustor will have been converted to NO_2.

The formation of nitric oxide (NO), proceeds at a high rate only at temperatures above about 1800 K [14]. NO is thus typically formed in the hot bulk flow region of the combustor and tends to be highest at full power conditions, where the flame temperature within the combustor is very high. Nitric oxide is formed by four different mechanisms: the Zeldovich mechanism, also known as the thermal mechanism, the prompt mechanism, the N_2O intermediate mechanism, and through fuel-bound nitrogen. The Zeldovich mechanism is a well known set of two chain reactions that

is extended by a third reaction.

$$O + N_2 \Leftrightarrow NO + N, \tag{4.1}$$

$$N + O_2 \Leftrightarrow NO + O, \tag{4.2}$$

$$N + OH \Leftrightarrow NO + H. \tag{4.3}$$

The reaction rate constants for the Zeldovich mechanism all have the Arrhenius form, which is given in Equation 4.4.

$$k(T) = AT^b exp(-E_A/R_u T), \tag{4.4}$$

where $k(T)$ is the reaction rate constant, which is only a function of temperature, A is a constant, T is the temperature, b is a constant, E_A is the activation energy, and R_u is the universal gas constant. Rate constants enter formation rate expressions of a chemical reaction like $A + B \Leftrightarrow C$, in the manner shown in Equation 4.5.

$$\frac{d[C]}{dt} = k(T)[A][B], \tag{4.5}$$

where $k(T)$ is the rate constant for the reaction and A and B are the concentrations of the reactants taking part in the reaction. The presence of the Arrhenius reaction rate constants in the Zeldovich mechanism reactions implies that the emissions of NO that result when the mechanism is dominant increase exponentially with temperature. Since the Zeldovich mechanism is dominant at high temperature, NO_x emissions should be increasing exponentially around temperatures of about 1800 K.

At lower temperatures the Zeldovich mechanism has a much smaller impact on NO formation and the prompt and N_2O intermediate mechanisms are responsible for most of the NO emissions. The prompt mechanism, which is linked to the combustion chemistry of hydrocarbons, occurs very rapidly in the flame zone of a reaction. In general terms, the prompt mechanism is due to hydrocarbon radicals reacting with N_2 to form intermediate compounds that ultimately become NO [17]. The chemical

reactions of the prompt mechanism are more complex and less well understood than the those of the Zeldovich mechanism. The N_2O intermediate mechanism is also responsible for some of the NO production at lower temperatures. The process tends to be important under fuel-lean conditions ($\phi_p < 0.8$) [17]. The chemistry of the N_2O mechanism is better understood than that of the prompt mechanism and is shown in Equations 4.6 through 4.8.

$$O + N_2 + M \Leftrightarrow N_2O + M, \tag{4.6}$$

$$H + N_2O \Leftrightarrow NO + NH, \tag{4.7}$$

$$O + N_2O \Leftrightarrow NO + NO, \tag{4.8}$$

where M is a third body. Since the prompt and N_2O intermediate mechanisms are prevalent at lower temperatures and the Zeldovich mechanism is nearly negligible, the emissions of NO_x should not follow the same exponential trend that they do at high temperature.

The final mechanism of NO_x formation is that due to fuel-bound nitrogen. Some fuels contain organically bonded nitrogen, which could eventually form NO [14]. This possibility was not included in the physics-based emissions model since the NO formation from fuel-bound nitrogen depends mainly on how much nitrogen is bonded to the fuel.

4.2 CO Chemistry

Hydrocarbon combustion can usually be characterized as a two-step process: first fuel is broken down to carbon monoxide, and second, carbon monoxide is oxidized to carbon dioxide [17]. This is shown as two global reactions in Equations 4.9 and 4.10 for propane.

$$C_3\ H_8 + 3.5O_2 \Rightarrow 3CO + 4H_2O, \tag{4.9}$$

$$CO + \frac{1}{2}O_2 \Leftrightarrow CO_2. \tag{4.10}$$

The chemistry involving CO is well understood (though it involves many minor species not shown), and the key difficulty in predicting CO emissions comes from the physical modeling of the combustor. This is because carbon monoxide emissions that result from incomplete combustion of the fuel are usually caused by three main sources that are difficult to account for [14]. These main sources for are:

1. Inadequate burning rates in the primary zone,
2. Inadequate mixing of the fuel and air,
3. Quenching of the postflame products by entrainment with the liner wall-cooling air.

CO emissions are sensitive to small changes in these conditions. Accurate prediction of CO emissions trends hinges on a model's ability to capture these three phenomena.

4.3 Predicting NO_x and CO Chemically

To determine whether or not the chemistry of combustion is captured correctly by the physics-based emissions model, the effects of the key inputs that impact combustion were studied. The inputs that have the most significant effect on combustion are the temperature and pressure of the combustor, as well as the primary zone equivalence ratio. These parameters are all inputs to the emissions model. Each of these parameters was varied with a range of $\pm$ 5% of the design value of the parameter at all four ICAO LTO-cycle conditions for Engine 1. The emissions indices of NO_x and CO were then calculated using the model and the results compared with theoretical arguments.

4.4 Model Response to T_3

Figure 4-1 gives the NO_x response of the model to combustor inlet temperature. The figure has three sets of data points corresponding from left to right, to the idle, approach, and takeoff conditions. The climb-out was not plotted in the figure for clarity.

The trends that should be compared to theoretical arguments are those found within each set of data points where the sensitivity of the model output to the variation of inlet temperature is established. The differences between the three sets of points contains changes in all parameters and not just inlet temperature and thus those differences do not provide an independent assessment of the impact of temperature. If the model is capturing the correct physics and chemistry, the high temperature NO_x emissions should trend exponentially with temperature. At the higher values of the combustor inlet temperature, for example, the takeoff condition, the NO_x levels are increasing exponentially with increases in temperature. At the lower temperature conditions, it is clear that the Zeldovich mechanism is not playing as prominent a role in NO_x formation since the trend does not follow the same exponential curve that it does at high temperature. This is the appropriate response. The results of the temperature analysis show that the model correctly estimates the general response of NO_x to temperature changes at the different power settings.

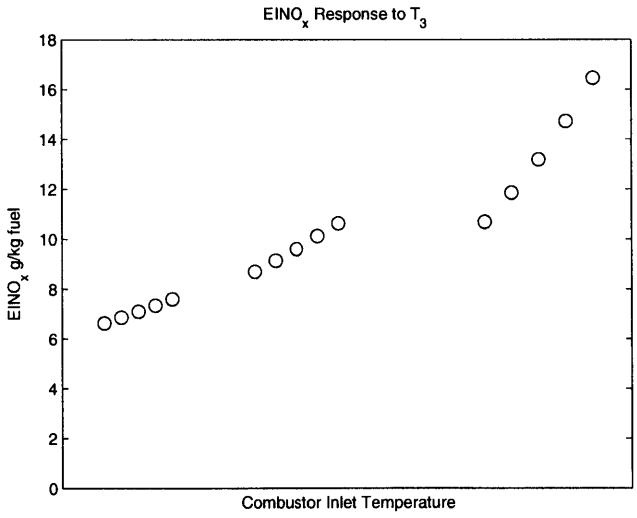

Figure 4-1: Model $EINO_x$ versus Combustor Inlet Temperature

Figure 4-2 gives the CO response of the model to combustor inlet temperature. The results for the figure were generated in the same way as the results for Figure 4-1. As mentioned previously, inadequate burning and mixing rates, as well as quenching of the reactions with cool air, lead to emissions of CO. In general, higher combustion

temperatures lead to faster burning rates, which should lead to lower emissions of carbon monoxide. If the emissions model is capturing the response of CO emissions with temperature correctly, CO emissions should decrease with increasing temperature. As shown in the figure, this is the case.

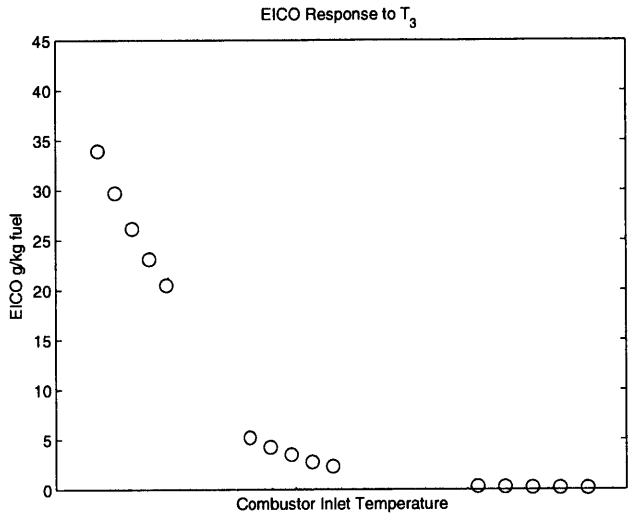

Figure 4-2: Model EICO versus Combustor Inlet Temperature

4.5 Model Response to P_3

The pressure at which combustion takes place is another factor that impacts the level of pollutants emitted from a combustor. As pressure increases, the flame temperature increases because higher pressures lead to lower dissociation losses [14]. The effect of increasing pressure on flame temperature is shown in Figure 4-3. Given that flame temperature has a significant effect on emissions of NO_x and CO, pressure changes should lead to predictable trends in emissions output.

Figure 4-4 shows the response of NO_x emissions to the combustor inlet pressure. Since liner pressure drop is nearly constant, varying inlet pressure was used as a surrogate for changes in combustor pressure [14]. Given that increasing pressure increases the flame temperature by a significant amount when pressures are initially low and by a smaller amount when pressures are higher, NO_x emissions, which generally in-

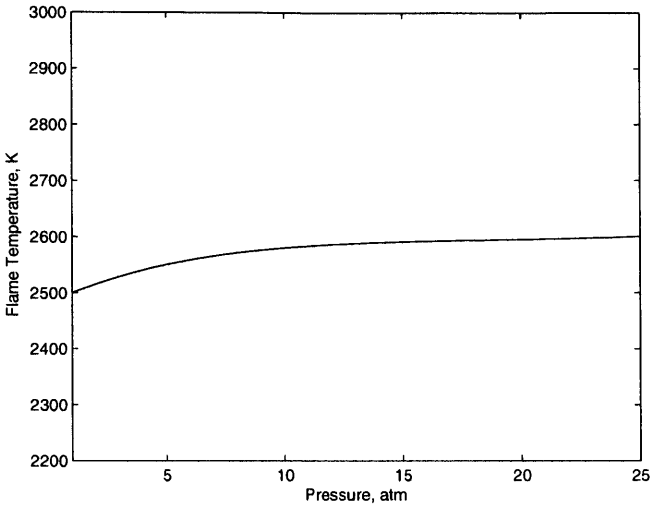

Figure 4-3: Effect of Pressure on Flame Temperature, adapted from [14]

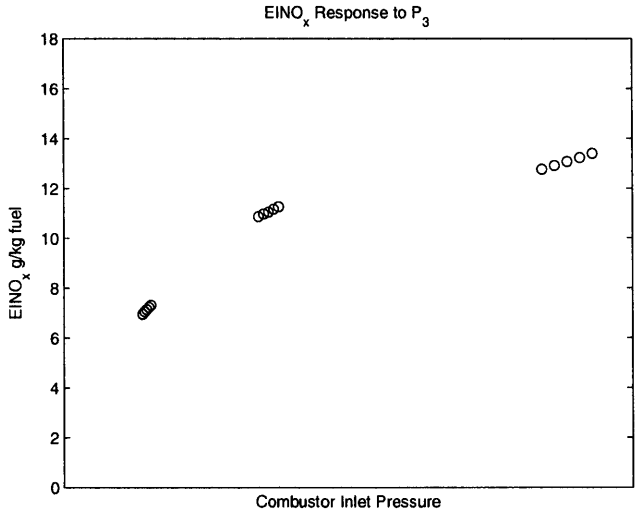

Figure 4-4: Model EINO$_x$ versus Combustor Inlet Pressure

crease with flame temperature, should show increases at all engine conditions, with the lower power conditions responding more strongly to pressure. Figure 4-4 shows that the model is capturing this response.

Figure 4-5 gives the response of the model CO emissions to increasing pressure. Since CO emissions generally decrease with flame temperature, pressure increases should lead to decreasing CO emissions. The effect should be more pronounced at

lower power than at higher power because of the effect of pressure on flame temperature. The model predicts this response.

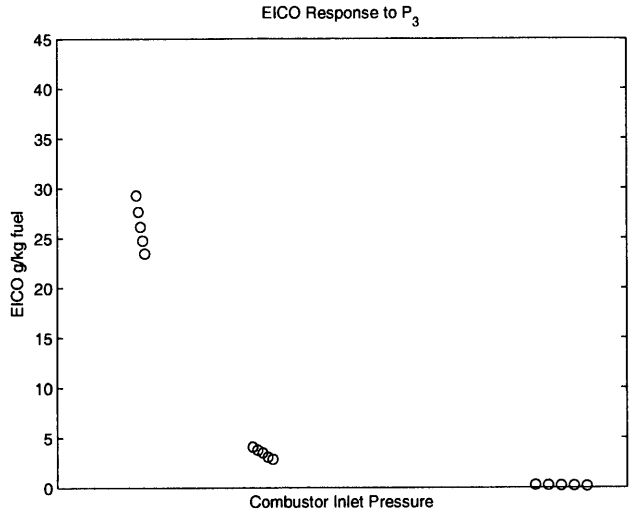

Figure 4-5: Model EICO versus Combustor Inlet Pressure

4.6 Model Response to Equivalence Ratio

The equivalence ratio of the primary zone of a combustor, which refers to the ratio of fuel and air to the stoichiometric ratio of fuel and air, has a strong effect on the flame temperature of combustion. The stoichiometric fuel-air ratio refers to the ratio of fuel and air at which all of the oxygen is used to oxidize all of the fuel, that is, there is no excess fuel or air in the mixture. Thus, as the fuel-air ratio becomes closer to the stoichiometric fuel-air ratio, meaning the equivalence ratio gets closer to unity, the temperature of the reactions increases significantly. This has a pronounced effect on the emissions of both NO_x and CO.

Figure 4-6 shows the response of the model NO_x emissions at idle and at climb-out to varying primary zone equivalence ratio. Approach and takeoff were not plotted for clarity. The primary zone equivalence ratio was varied $\pm 5\%$ at both idle and climb-out by varying the fuel flow into the primary zone. The figure shows that as the equivalence ratio is brought closer to unity, the emissions of NO_x increase. This is

the appropriate result since the flame temperature increases as the equivalence ratio moves closer to unity.

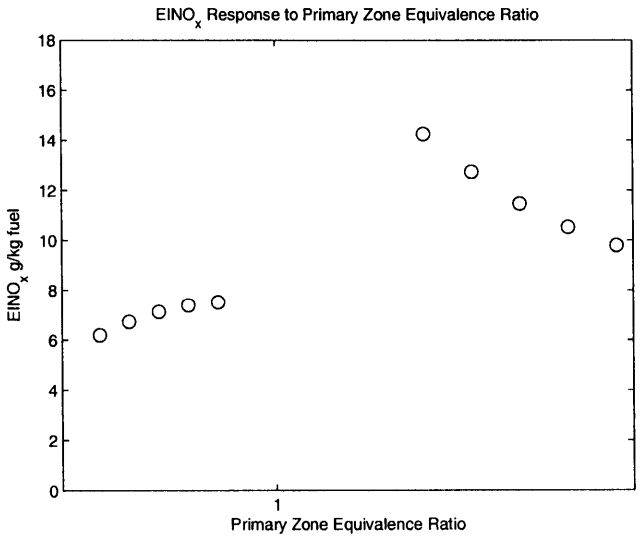

Figure 4-6: Model EINO$_x$ versus Primary Zone Equivalence Ratio

Figure 4-7 gives the response of the model CO emissions at idle and climb to varying primary zone equivalence ratio. The results were produced in the same way as they were for Figure 4-6. At the idle condition, where large amounts of CO are anticipated, the effect of increasing equivalence ratio has a significant impact on CO emissions. The increasing flame temperatures caused by increasing the equivalence ratio causes a reduction in CO emissions. The climb-out condition reveals a weaker response of CO to increasing equivalence ratio. At this condition, the temperatures are high and the varying equivalence ratio does not reduce the temperature enough to have a significant impact on CO. This is consistent with what the model should be estimating.

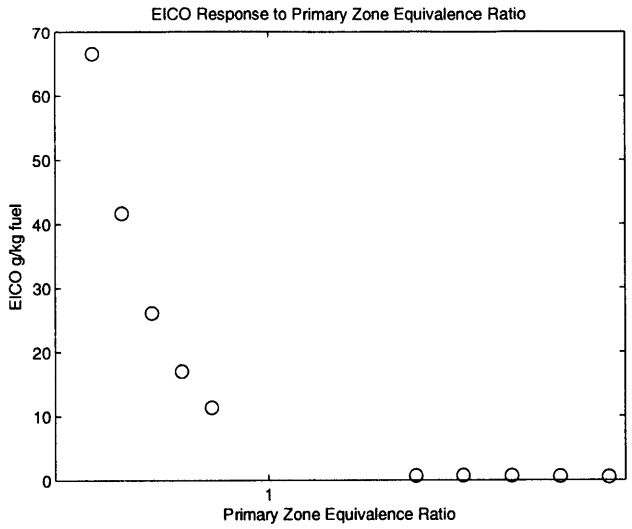

Figure 4-7: Model EICO versus Primary Zone Equivalence Ratio

4.7 Capturing the Effects of Gas Turbine Combustor Design

Most of the discussion thus far regarding the response of NO_x and CO emissions has been based on the correct modeling of the chemical processes taking place within the combustor. The physics-based emissions model however, must also account for the physical layout of a gas turbine combustor and how that affects the combustion that takes place. To determine if the model is capturing the physics and chemistry along the length of the combustor, the emissions output from each zone was studied for each ICAO LTO-cycle power setting.

4.7.1 Idle Emissions Output

Figure 4-8 shows the NO_x and CO emissions in grams that are produced or oxidized in each zone of the model of an industry combustor at the idle power setting. For NO_x, nearly all of the production occurs in the primary zone of the combustor as anticipated given that the temperatures are highest in the primary zone, and that at idle power, the temperature is quickly reduced below the value of about 1800

K in the intermediate zone. For CO, formation occurs in the primary zone where

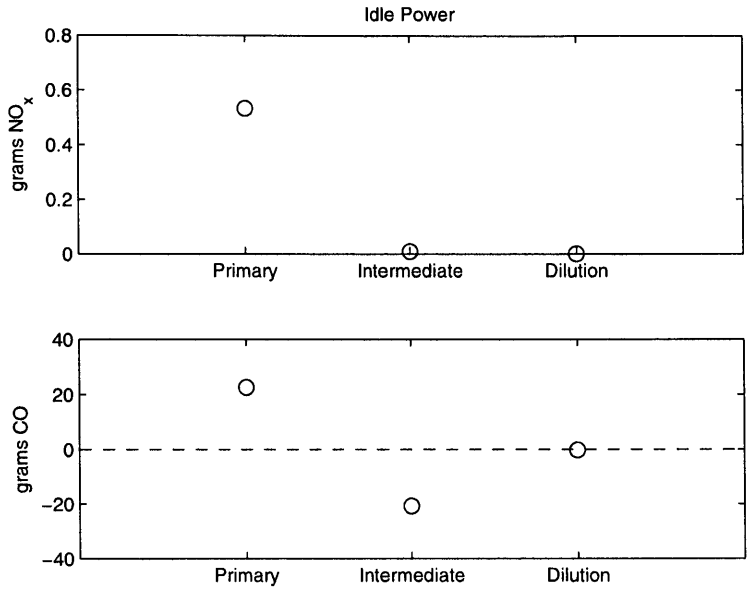

Figure 4-8: Model Combustor Zone Emissions Production at Idle Power

dissociation losses from the combustion result in CO that has yet to oxidize to CO_2. The intermediate zone, which is designed to recover the dissociation losses of the primary zone, is shown in the figure to oxidize most of the CO that was formed in the primary zone. The dilution zone has little effect on both NO_x and CO, which is appropriate because at that point in the combustor most of the reactions have taken place and the dilution zone serves to only reduce the mean gas temperature prior to the turbine. The results for the idle power setting show that the model combustor zones capture the expected behavior of the emissions production and destruction within the physical combustor.

4.7.2 Approach Emissions Output

Figure 4-9 gives the NO_x and CO emissions for each zone for the approach power setting. NO_x is again produced almost entirely in the primary zone of the model. This is consistent with the physical nature of the combustor at this power setting. CO is again formed in the primary zone in great quantities due to dissociation and

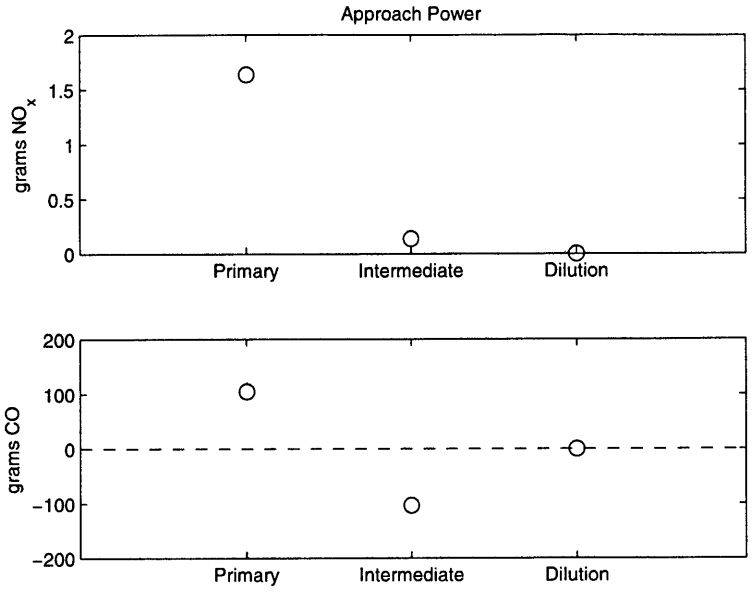

Figure 4-9: Model Combustor Zone Emissions Production at Approach Power

oxidized in the intermediate zone. The dilution zone is again having little effect on the emissions outputs. The approach condition reveals that the CO formed in the primary zone is greater than that formed in the primary zone at the idle condition. This is consistent with CO kinetics. As shown in Figure 4-10, at low equivalence ratios, CO oxidation does not reach the equilibrium value of CO. As equivalence ratio is increased however, CO levels approach equilibrium in the primary zone. For the range of equivalence ratios typically found in the primary zone of a gas turbine combustor, (about 0.6 to 1.8), the non-equilibrium CO values can be lower than CO levels at higher equivalence ratios where CO is at its equilibrium value. This is the case for the equivalence ratios of the industry combustor at idle and approach. Thus, even though the CO emissions from gas turbine combustors are higher at idle than they are at higher power settings, the CO emissions from the primary zone of the combustor are lower at idle in some cases than at higher power. The model estimates this correctly.

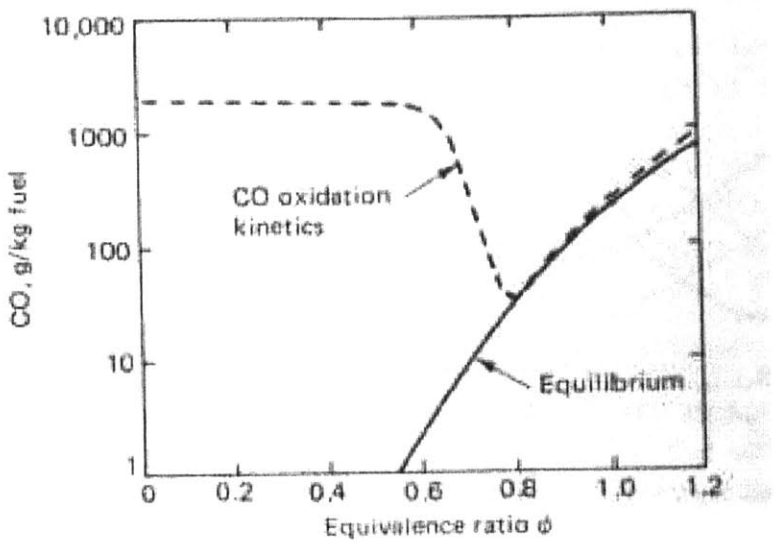

Figure 4-10: Carbon Monoxide Emissions versus Primary Zone Equivalence Ratio [14]

4.7.3 Climb-Out Emissions Output

The results of the climb-out power setting emissions outputs from each zone of the model were similar to those of the idle and approach settings and are shown in Figure 4-11. The NO_x emissions are mainly from the primary zone, though the intermediate zone is shown to be producing some NO_x. This is due to the higher temperature conditions at this power setting and is an appropriate result. The CO emissions follow the same trend as they did for the other power settings. CO is formed in the primary zone and oxidized in the intermediate zone. The CO is again attaining an equilibrium value in the primary zone that is higher than that of the approach setting. This is consistent with Figure 4-10 given that the climb-out condition has a higher primary zone equivalence ratio than the approach condition.

4.7.4 Takeoff Emissions Output

The takeoff results are also similar to the other power settings and are shown in Figure 4-12. The intermediate NO_x production is higher still at takeoff, which is consistent with the fact that the temperatures are highest at this condition and the interme-

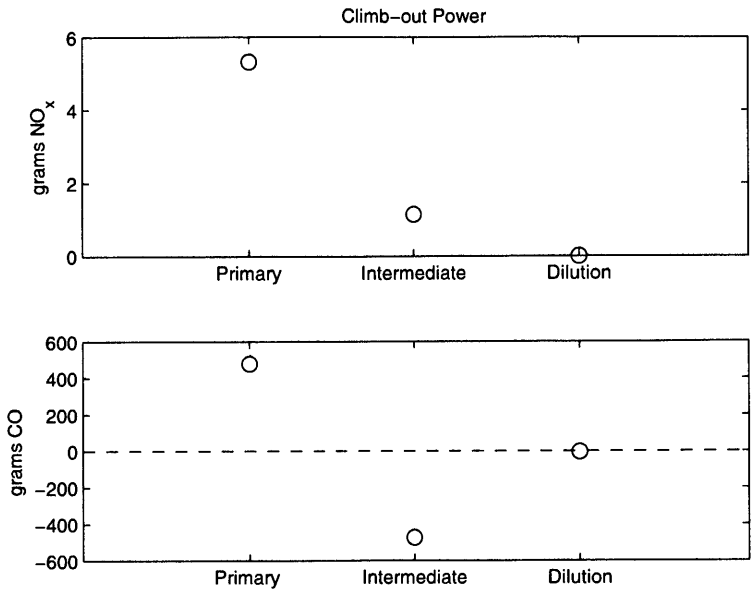

Figure 4-11: Model Combustor Zone Emissions Production at Climb Out Power

diate zone temperature has not been reduced enough to halt NO_x formation. CO

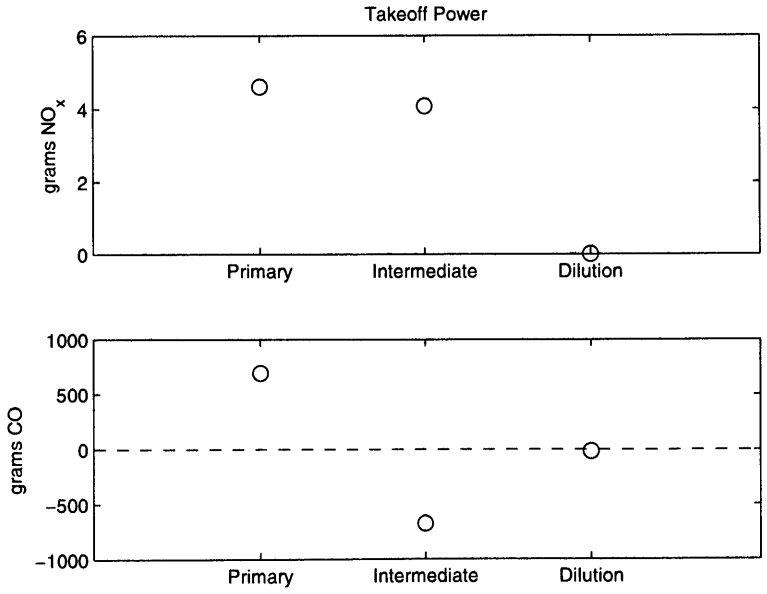

Figure 4-12: Model Combustor Zone Emissions Production at Takeoff Power

emissions in the primary zone are highest at takeoff as expected from the discussion

on equivalence ratio and CO equilibrium.

4.7.5 Assessment of Model Capability

The model was shown to correctly capture trends in emissions outputs. The responses to temperature, pressure and equivalence ratio were appropriate and the production and oxidation of emissions within the various zones of the model match those expected for an example industry combustor. Confidence in the model's ability to represent the physical relationships between operating conditions, design parameters, and pollutant emissions in a consistent manner has thus been established.

Chapter 5

Results

This chapter presents results generated by the model using industry data for the five combustors discussed previously. The results include emissions estimates from the model for Engines 1, 2, and 3, the model estimates of the effects of the design changes from Engine 1 to Engine 1a and Engine 3 to Engine 3a. Also included is a model estimate of NO_x and CO emissions for a full throttle sweep of Engine 1a. The results are all discussed in the context of the objectives of the model as described in sections 1.4 and 2.1.

5.1 Model Predictions for Engines 1, 2, and 3

Using the individually set unmixedness curve fit for Engines 1, 2, and 3, the model was run using the input data for the four ICAO LTO-cycle points and the predictions for NO_x and CO were compared to the ICAO certification data. The NO_x predictions are also compared to predictions from the NPSS single-annular combustor NO_x empirical model given in Equation 1.4, to determine how well the model performs relative to an empirical model at predicting trends in the emission levels of different combustor designs.

5.1.1 Overview of the Results

The use of the model to predict the emissions of NO_x and CO from Engines 1, 2, and 3 revealed that the NO_x estimates from the model were better than the estimates from the empirical model for most cases, with the exception of the idle condition for each engine, which was predicted poorly by both the physics-based model and the empirical model. For CO emissions, the physics-based model estimates idle CO, which is the dominant contribution to CO Dp/Foo, within the uncertainty bounds for all three engines. At higher power the model does not perform as well, estimating most of the approach, climb-out, and takeoff CO levels outside of the uncertainty bounds. For all three engines however, the CO Dp/Foo is estimated within the uncertainty bounds, owing to the dominance of idle CO and the model's ability to estimate it within the uncertainty in the data for these engines.

5.1.2 Engine 1 Estimates

The results of the model estimates for Engine 1 are shown in Figure 5-1. Figure 5-1a is a comparison of the model estimated $EINO_x$ with the ICAO certification data and the empirical model estimate. The whiskers on the ICAO data points cover the $\pm 16\%$ uncertainty in the certification data. For Engine 1, the physics-based model estimates the NO_x emissions at approach, climb-out, and takeoff better than the empirical model. Neither the physics-based model nor the empirical model estimate idle NO_x well. Figure 5-1b, is a comparison of the model estimated EICO with the ICAO certification data. The whiskers on the ICAO points are the $\pm 23\%$ uncertainty in the EICO certification data. There is no comparison to an empirical model because, as mentioned previously, there are no non-proprietary empirical CO models. The figure shows that the model estimates the emissions of CO from Engine 1 within the uncertainty in the ICAO certification data for both idle and approach. Takeoff and climb-out CO estimates for Engine 1 are outside of the uncertainty in the data, which is unclear from the figure due to the low EICO values at those conditions. Figure 5-1c, is a comparison of the model estimated Dp/Foo for NO_x with the ICAO certification

value as well as the empirically estimated value, and the model estimated Dp/Foo for CO with the ICAO certification value. The whiskers are again the uncertainty in the NO_x and CO ICAO certification data. The figure shows that the model estimates both the NO_x and CO Dp/Foo from Engine 1 within the uncertainty bounds. The figure also shows that the empirical model estimated the NO_x Dp/Foo within the uncertainty bounds.

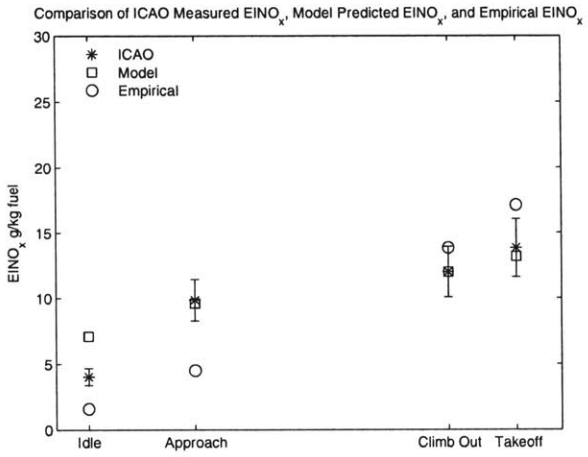

(a) $EINO_x$

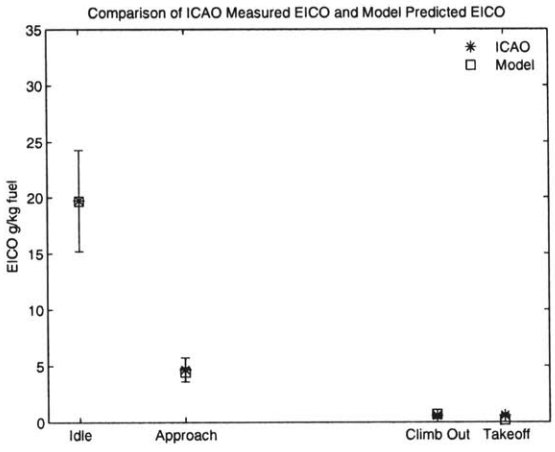

(b) EICO

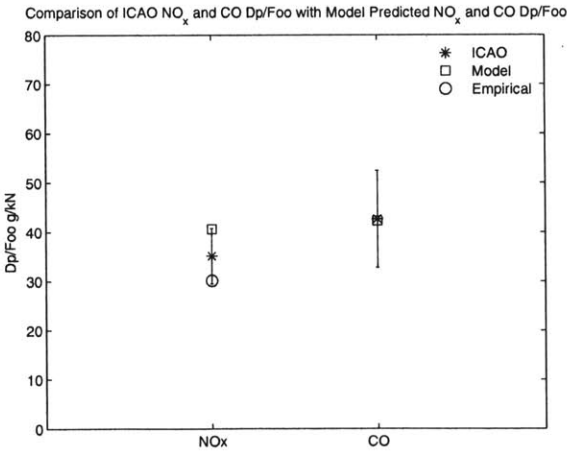

(c) Dp/Foo

Figure 5-1: Emissions Estimates for Engine 1

5.1.3 Engine 2 Estimates

The results of the model estimates for Engine 2 are shown in Figure 5-2. The plots give the $EINO_x$, EICO, and Dp/Foo estimates of the model compared to the ICAO certification data and the empirical model estimates where applicable. The physics-based model estimates the NO_x emissions at approach, climb-out, and takeoff within the ICAO uncertainty in the data and does a poor job estimating the NO_x at idle. The empirical model estimates the climb-out condition within the uncertainty in the data but not the idle, approach, or takeoff condition. The EICO model estimate for Engine 2, shown in Figure 5-2b, is within the uncertainty in the data at the idle condition and outside of the uncertainty in the data at approach, climb-out, and takeoff. The Dp/Foo estimate for NO_x, shown in Figure 5-2c, is outside of the uncertainty band for both the physics-based model and the empirical model. The Dp/Foo estimate for CO, also shown in Figure 5-2c, is within the uncertainty in the CO certification data.

5.1.4 Engine 3 Estimates

The results for Engine 3 are shown in Figure 5-3. The plots are for $EINO_x$, EICO, and Dp/Foo for NO_x and CO, as they were in Figures 5-1 and 5-2. Figure 5-3a, shows that the model is estimating NO_x emissions within the uncertainty bounds at climb-out and takeoff and is not predicting NO_x emissions within the uncertainty in the data at idle and approach. The same is true for the estimates from the empirical NO_x model. Figure 5-3b, shows that estimate of idle EICO is within the uncertainty in the data but the approach EICO estimate is not. The climb-out and takeoff conditions are also estimated outside of the uncertainty bounds, which is not shown clearly in the figure. The Dp/Foo estimates for NO_x and CO are shown in Figure 5-3c. The model estimates both the NO_x and CO Dp/Foo within the uncertainty bounds. The empirical NO_x model also estimates the Dp/Foo for NO_x within the uncertainty in the data.

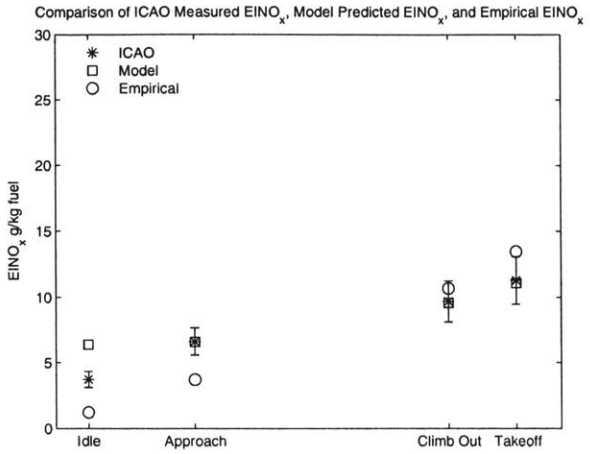

(a) EINO$_x$

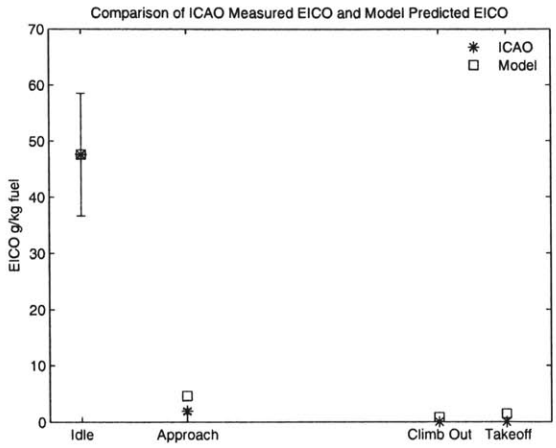

(b) EICO

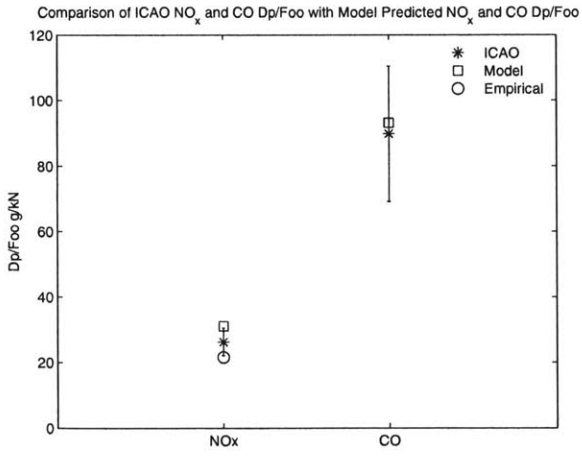

(c) Dp/Foo

Figure 5-2: Emissions Estimates for Engine 2

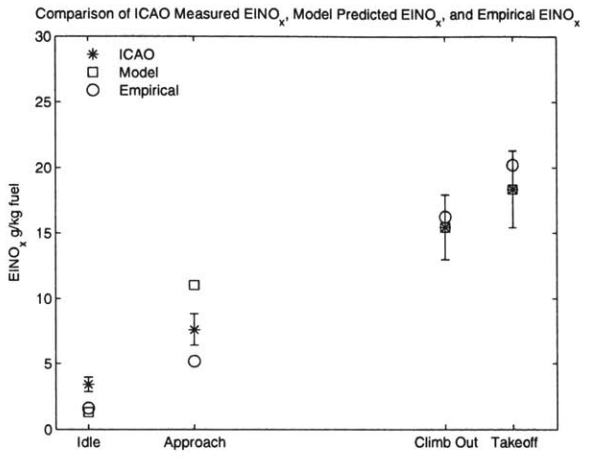

(a) EINO$_x$

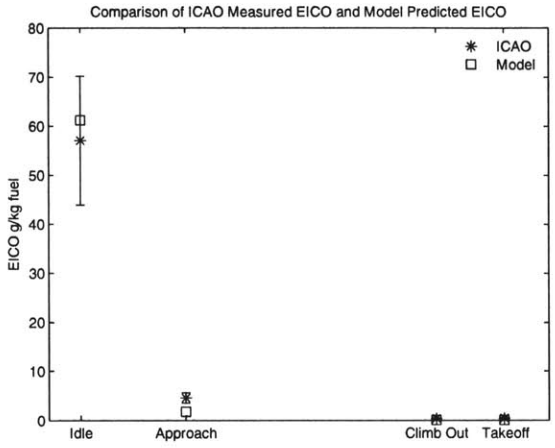

(b) EICO

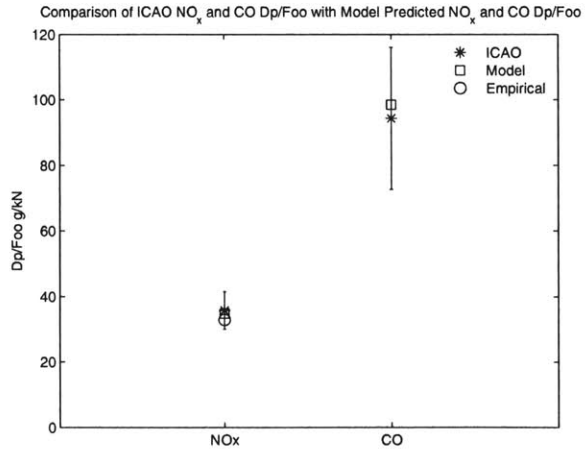

(c) Dp/Foo

Figure 5-3: Emissions Estimates for Engine 3

5.1.5 Overall Estimates

Figure 5-4 shows the estimates from the model of $EINO_x$ and EICO for all three engines. The figure also includes the empirical NO_x model estimates for all three engines. The solid line is the line of exact match between the estimated and the certification data emissions of NO_x and CO. The dashed lines are the uncertainty bounds for each emission. The plus marks on the figure are the model estimated NO_x and CO values and the circles are the empirical model estimated NO_x values. The figure shows that the estimated NO_x emissions from the model are closer to the

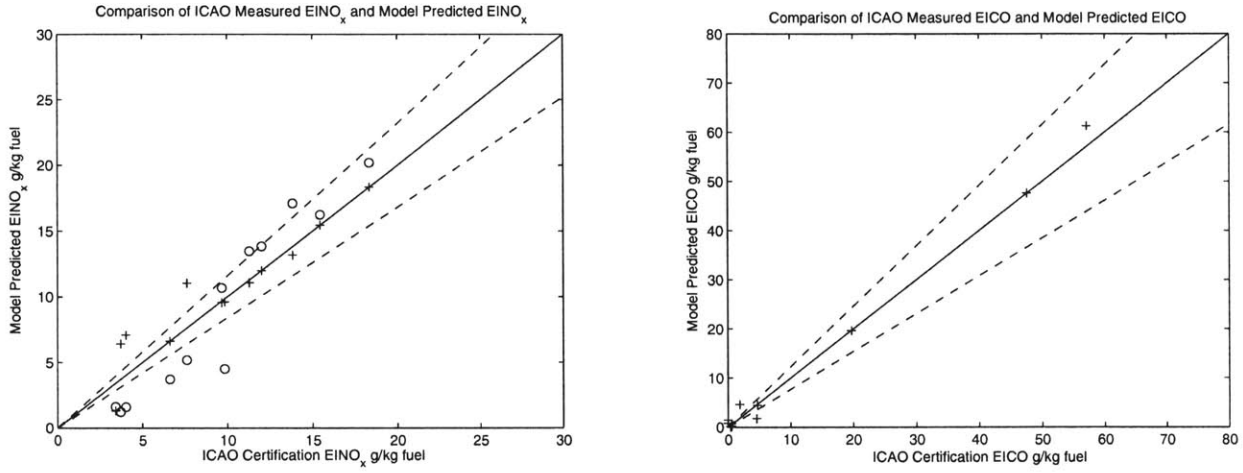

(a) $EINO_x$ (b) EICO

Figure 5-4: Emissions Estimates for Engines 1, 2, and 3

ICAO certification data than the empirical model in most cases. The lower values of $EINO_x$ (below 5 g/kg fuel on the figure), where both the model and the empirical model are outside of the uncertainty bands, are the idle conditions where neither model performs well. The figure also shows that the estimated CO emissions from the model are within the uncertainty bands for the higher values of EICO, which make the most significant contributions to CO Dp/Foo.

5.1.6 Discussion of Engine 1, 2, and 3 Model Estimates

From Figures 5-1, 5-2, 5-3, and 5-4, it is clear that the estimates of NO_x emissions are as good or better than those of the empirical model at nearly all conditions. The only exception is the low power condition, where both the physics-based model and the empirical model do a poor job. This is likely due to the complex NO_x chemistry that may not be modeled appropriately in the physics-based model at lower temperature and due to the emphasis on the Zeldovich mechanism, which is not dominant at low power, in the empirical model. For these three engines the model is thus meeting the objective of performing as well as an empirical NO_x model at predicting trends across different engine designs and operating conditions.

The figures also show that the model estimates low power emissions of carbon monoxide well, since all idle estimates were within the uncertainty bounds for CO. The CO emissions at higher power levels are not estimated as well by the model but, since these higher power conditions produce low emissions of CO relative to idle CO, the Dp/Foo estimates are within the uncertainty in the data. For these three engines the model is thus meeting the objective of predicting CO Dp/Foo levels within the uncertainty in the data.

5.2 Predicting the Effects of Design Changes

An objective of physics-based emissions model is to predict broad trends in pollutant emissions using a single methodology across different combustor designs and operating conditions using only high-level parameters. The following results assess the performance of the model in terms of meeting that objective through the model estimates of the effects of two design changes on the emissions of NO_x and CO.

5.2.1 Overview of Results

The results for both design changes were obtained by using the individually set unmixedness curves discussed in Chapter 3. For the design change from Engine 1a to

Engine 1, the emissions model performs better than the empirical model at estimating individual levels of NO_x at the four LTO-cycle points. The empirical model performs better than the physics-based model at estimating the NO_x Dp/Foo change between the two engines, but this is due to error cancellations between the certification points when they are summed in the Dp/Foo metric. The CO predictions from the model are outside of the uncertainty in the data for most of the certification points for the two engines, but the change in CO Dp/Foo from Engine 1a to Engine 1 is captured correctly.

For the design change from Engine 3 to Engine 3a, the emissions model performs as well as the empirical model in terms of NO_x estimates. The CO estimates from the model are outside of the uncertainty in the data for most conditions for Engines 3 and 3a, but the change in Dp/Foo between the two engines is captured within the uncertainty in the data by the model.

5.2.2 Engine 1a to Engine 1

Table 5.1 compares the model estimated NO_x emissions for Engine 1a with the ICAO certification data and the empirically estimated NO_x emissions at the four LTO-cycle points. The model estimates of NO_x are all within $\pm 16\%$ uncertainty with

	ICAO	Model	Empirical
	$EINO_x$ g/kg fuel	$EINO_x$ g/kg fuel	$EINO_x$ g/kg fuel
Idle	4.43	1.40	1.53
Approach	11.26	12.15	5.01
Climb Out	14.30	14.15	18.32
Takeoff	19.19	19.58	24.19

Table 5.1: Engine 1a NO_x Emissions

the exception of the idle setting. None of the empirical estimates are within the uncertainty in the certification data. Table 5.2 compares the model estimated CO emissions for Engine 1a with the ICAO certification data. The model estimates for CO are all outside the $\pm 23\%$ uncertainty with the exception of approach, with the idle CO being overestimated by 82%. Idle CO can be estimated within the uncertainty

for all engines studied in the this research with the exception of Engine 1a. This issue will be discussed in more detail in Chapter 6.

	ICAO	Model
	EICO g/kg fuel	EICO g/kg fuel
Idle	20.12	36.66
Approach	4.09	3.53
Climb Out	0.62	0.17
Takeoff	0.92	0.12

Table 5.2: Engine 1a CO Emissions

For the analysis of the design change from Engine 1a to Engine 1, the results for Engine 1a are considered baseline values. How well the model captures the effects of the design change is assessed by comparing how the estimated emissions levels change at each condition between the two engines with the certification data for the two engines. Table 5.3 compares the certification NO_x data for Engine 1 with the model estimated and the empirically estimated NO_x emissions. The model estimates

	ICAO	Model	Empirical
	$EINO_x$ g/kg fuel	$EINO_x$ g/kg fuel	$EINO_x$ g/kg fuel
Idle	4.03	7.12	1.59
Approach	9.85	10.94	4.50
Climb Out	12.00	11.29	13.83
Takeoff	13.82	13.00	17.10

Table 5.3: Engine 1 NO_x Emissions

the approach, climb-out, and takeoff condition within the uncertainty in the data. The empirical model does not estimate the NO_x emissions at any condition within the uncertainty in the data. The response of the certification emissions levels to the design change from Engine 1a to Engine 1 was a decrease in NO_x emissions at all of the certification points. The model NO_x emissions response to the design change was a decrease in NO_x emissions at approach, climb-out, and takeoff, and an increase in NO_x emissions at idle. The empirical model response to the design change was also a decrease in NO_x emissions at approach, climb-out, and takeoff, and an increase in NO_x emissions at idle. Table 5.4 shows the calculated NO_x Dp/Foo values for Engines 1a and 1 from the certification data, the model, and the empirical model.

The certification data shows a decrease in NO_x Dp/Foo of about 24% as a result of the design change. The physics-based model estimates a decrease of about 3% in NO_x Dp/Foo. The empirical model estimates a decrease of about 34%. Given that

	ICAO	Model	Empirical
	NO_x g/kN	NO_x g/kN	NO_x g/kN
Engine 1a	46.56	42.08	45.49
Engine 1	35.16	40.76	30.16

Table 5.4: Engine 1a and Engine 1 NO_x Dp/Foo Estimates

a change of 24% in certification Dp/Foo is greater than the uncertainty in the data, the change in Dp/Foo is signficant and was not captured by the physics-based model. This is due to the idle NO_x estimates. The empirical model appears to capture the change in NO_x Dp/Foo correctly however, given that the emissions of NO_x at each certification point was estimated outside of the uncertainty in the data, the estimate was the result of the errors in the four separate estimates at the certification points cancelling out and thus should not be taken as a positive result for the empirical modeling method.

Table 5.5 compares the certification CO data for Engine 1 with the model estimated CO emissions at the four certification points. The model estimates climb-out CO within the uncertainty in the data and idle, approach, and takeoff outside of the uncertainty in the certification data. Table 5.6 compares the certification data CO

	ICAO	Model
	EICO g/kg fuel	EICO g/kg fuel
Idle	19.73	26.66
Approach	4.67	3.56
Climb-Out	0.57	0.69
Takeoff	0.59	0.21

Table 5.5: Engine 1 CO Emissions

Dp/Foo with the model estimated CO Dp/Foo for Engines 1a and 1. The model estimates a decrease of about 15% in CO Dp/Foo from Engine 1a to Engine 1, while the certification data gives an increase of about 11% from Engine 1a to Engine 1. The change in CO Dp/Foo in the certification data from Engine 1a to Engine 1 is within

the uncertainty in the data and therefore is not significant. The model estimate, which is a change of less than 23%, is thus appropriate.

	ICAO	Model
	CO g/kN	CO g/kN
Engine 1a	38.52	65.10
Engine 1	42.67	55.30

Table 5.6: Engine 1a and Engine 1 CO Dp/Foo Estimates

5.2.3 Discussion of the Engine 1a to Engine 1 Design Change Results

One of the objectives of the model is to predict broad trends in emissions levels from different combustor designs within the uncertainty in the certification data for CO and as well as empirical models for NO_x. The change in CO Dp/Foo was captured correctly because there was no significant change in the certification data (meaning the change was within the uncertainty in the data) and the model estimated this. However, the model did not estimate the emissions levels of CO at the individual certification points within the uncertainty in the data with the exception of climb-out for Engine 1 using the Engine 1a derived unmixedness curve. The objective for CO emissions prediction was therefore, not met for this design change but the results are promising because the objective of predicting the correct sign for changes in CO emission with changing design and operating parameters was met.

For NO_x emissions, the model estimates the emissions levels within the uncertainty in the data for all but the idle condition, but does not capture the magnitude of the change in NO_x Dp/Foo. The empirical model does not estimate the emissions levels within the uncertainty in the data for any condition, but it does capture the change in NO_x Dp/Foo within the uncertainty in the data. However, this was the result of error cancelling among the four certification points. The objective for NO_x emissions prediction therefore, was not met because the model did not perform as well as the empirical model in terms of the NO_x Dp/Foo, but given that the only weakness of

the model for NO_x emissions appears to be predicting idle NO_x, the results for NO_x are also promising.

Another objective of the model is to include high-level design parameters and operating conditions that would be convienient for an expert to use in projecting future technology. Figure 5-5 shows the percentage changes in the model inputs for the design change from Engine 1 to Engine 1a. The inputs shown in the figure are the only elements of the model that were changed between the two engines. Since the results of the design change from Engine 1a to Engine 1 were promising both in terms of NO_x and CO, the possibility of creating a model using only high-level, convienient parameters is plausible.

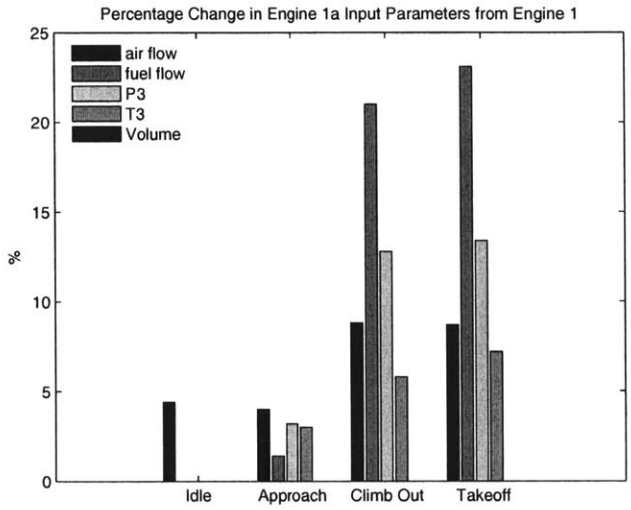

Figure 5-5: Percentage Change of Inputs from Engine 1 to Engine 1a

5.2.4 Engine 3 to Engine 3a

Tables 5.7 and 5.8 show the model and empirical estimates of NO_x emissions for Engine 3 compared to the ICAO certification data and the model estimates of CO emissions for Engine 3 compared to the ICAO certification data. The model NO_x estimates are within the uncertainty in the data for climb-out and takeoff and outside of the uncertainty for idle and approach. The empirical model estimates are also

	ICAO	Model	Empirical
	$EINO_x$ g/kg fuel	$EINO_x$ g/kg fuel	$EINO_x$ g/kg fuel
Idle	3.42	1.31	1.61
Approach	7.63	11.04	5.18
Climb-out	15.44	15.44	16.23
Takeoff	18.34	18.34	20.19

Table 5.7: Engine 3 NO_x Emissions

within the uncertainty in the data for climb-out and takeoff and outside of the uncertainty for idle and approach. The model CO estimate for the idle condition is within the uncertainty in the data for Engine 3 and not within the uncertainty at any other condition. The assessment of the model's ability to capture the effects of the design change from Engine 3 to Engine 3a is based on how the changes in the emissions values in the certification data are captured by the model. The certification data and model estimates for Engine 3a are shown in Tables 5.7 and 5.8. Table 5.9 compares

	ICAO	Model
	EICO g/kg fuel	EICO g/kg fuel
Idle	57.06	61.22
Approach	4.57	1.76
Climb-out	0.37	0.07
Takeoff	0.42	0.05

Table 5.8: Engine 3 CO Emissions

the certification NO_x data for Engine 3a with the model estimated and the empirically estimated NO_x emissions. The model estimates idle, climb-out, and takeoff NO_x within the uncertainty in the data. The empirical model estimates only climb-out and takeoff within the uncertainty in the data. From Engine 3 to Engine 3a, the certification NO_x emissions levels for all four ICAO LTO-cycle points increased. This result is estimated correctly by the physics-based emissions model and the empirical NO_x model. Table 5.10 shows the calculated Dp/Foo values for Engines 3 and 3a from the certification data, the model, and the empirical model. The certification data NO_x Dp/Foo increases about 9%, the model NO_x Dp/Foo increases by about 20%, and the empirical model NO_x Dp/Foo increases by about 12%. Both the physics-based model and the empirical model estimate the change in NO_x Dp/Foo between Engines

	ICAO	Model	Empirical
	$EINO_x$ g/kg fuel	$EINO_x$ g/kg fuel	$EINO_x$ g/kg fuel
Idle	3.59	4.12	1.74
Approach	8.02	11.23	5.59
Climb-out	16.68	17.01	17.98
Takeoff	20.40	19.28	22.68

Table 5.9: Engine 3a NO_x Emissions

3 and 3a within the uncertainty in the certification data. Table 5.11 compares the

	ICAO	Model	Empirical
	NO_x g/kN	NO_x g/kN	NO_x g/kN
Engine 3	35.81	34.85	32.90
Engine 3a	39.03	41.98	36.78

Table 5.10: Engine 3 and Engine 3a NO_x Dp/Foo Estimates

certification CO data for Engine 3a with the model estimated CO emissions at the four LTO-cycle points. The model does not estimate the CO emissions at any of the four points within the uncertainty in the certification data. Table 5.12 compares

	ICAO	Model
	EICO g/kg fuel	EICO g/kg fuel
Idle	49.94	68.33
Approach	3.68	0.80
Climb-out	0.38	0.05
Takeoff	0.52	0.06

Table 5.11: Engine 3a CO Emissions

the certification data CO Dp/Foo with the model estimated CO Dp/Foo for Engines 3 and 3a. The model estimates an increase of about 9% in CO Dp/Foo while the certification data contains a decrease of about 14%. There is therefore a negligible change in CO Dp/Foo given the uncertainty in the data, which is estimated correctly by the model.

	ICAO	Model
	CO g/kN	CO g/kN
Engine 3	94.35	98.50
Engine 3a	81.49	107.73

Table 5.12: Engine 3 and Engine 3a CO Dp/Foo Estimates

5.2.5 Discussion of the Engine 3 to Engine 3a Design Change Results

The effect of the design change from Engine 3 to Engine 3a on NO_x emissions is captured by the physics-based model as well as or better than the empirical model for all cases. The emissions model thus meets the objective of predicting NO_x emissions as well as an empirical model for this particular design change. The effect of the design change on CO emissions is captured by the model within the uncertainty in the data in terms of CO Dp/Foo, but the results are not as good for the individual data points. The objective of predicting CO emissions within the uncertainty in the data was therefore, not met for this particular design change, but the results were again promising.

Figure 5-6 gives the percentage changes to the input parameters of the model from Engine 3 to Engine 3a. Using only these parameter changes the model predicted NO_x

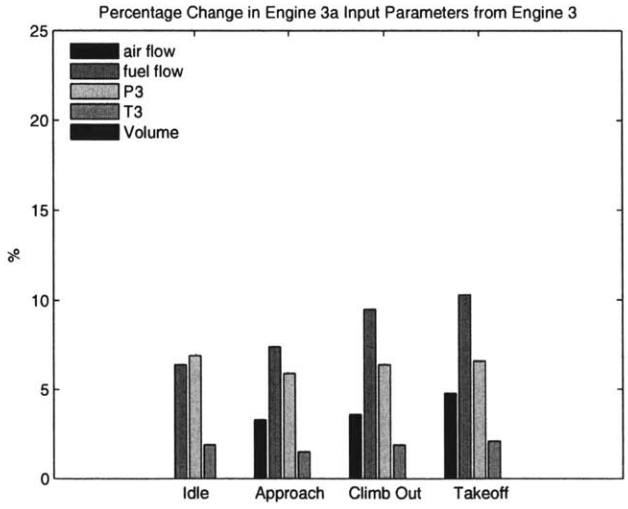

Figure 5-6: Percentage Change of Inputs from Engine 3 to Engine 3a

emissions better than the empirical model and CO Dp/Foo within the uncertainty in the data, meeting the objective of using high-level, convienient design parameters and operating conditions in the model.

5.3 NO_x Estimates for a Full Throttle Sweep

To assess the model's ability to consistently capture the effect of combustor operating conditions on pollutant emissions, a full throttle sweep of operating conditions for Engine 1a was run with the model and the results were compared to data collected during the engine's certification testing. To show the benefit of capturing the effects of operating conditions on pollutant emissions, the model estimates for NO_x and CO are compared with the estimates from the Boeing fuel flow method 2 (BM2), which is a widely used method for modeling emissions of NO_x and CO at different operating conditions [12].

5.3.1 Throttle Sweep Emissions Estimates

Figure 5-7 compares the emissions model estimates with the data collected on Engine 1a during certification testing for NO_x and CO. The empirical NO_x model results are also shown. The figure shows that the NO_x estimates of the model follow the trend in the certification data more closely than the empirical model. The physics-based emissions model is therefore capturing the relationship between operating conditions and NO_x emissions better than the empirical model.

The CO estimate from the model follows the same trend as the test CO data but at low fuel flow rates the CO estimates from the model are significantly higher than the test data values. The uncertainty is not shown on the plot but the CO estimates at these low power conditions are not within the uncertainty in the data. The physical relationship between CO emissions and operating conditions however is captured because the trend is estimated correctly.

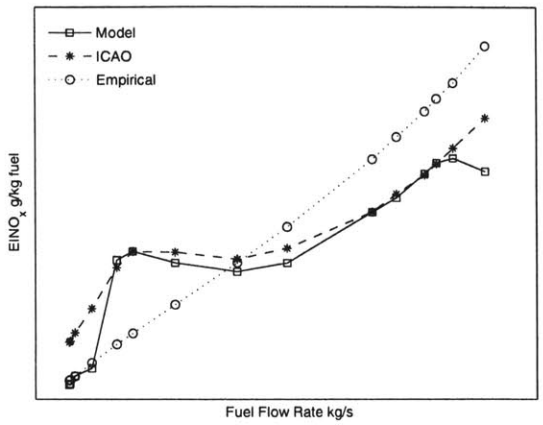

(a) EINO$_x$

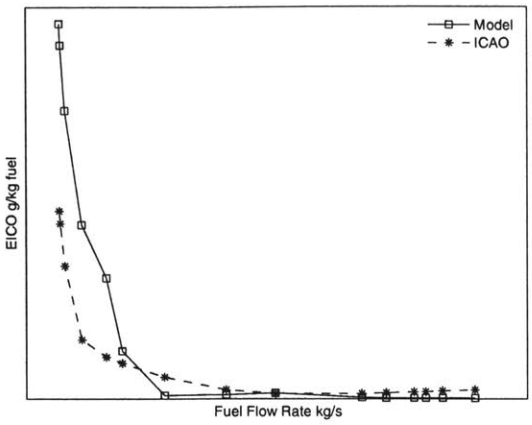

(b) EICO

Figure 5-7: Throttle Sweep Emissions Estimates for Engine 1a

5.3.2 Throttle Sweep Estimates versus Boeing Fuel Flow Method 2

The Boeing fuel flow method 2 uses emissions indices of NO_x and CO and corresponding fuel flows at the ICAO certification points to model emissions at different engine operating conditions. For NO_x, the values of the emissions index at the ICAO points are plotted against the fuel flow rates at those engine conditions. Values of EINO$_x$ at other operating conditions are then determined with linear interpolations between LTO-cycle points. For CO, the same technique is used but only two linear interpolations are used, one between idle and approach and one between climb-out and takeoff. The two linear interpolations form a corner that is usually between the approach and climb-out conditions.

Figure 5-8 shows the BM2 estimates of EINO$_x$ and EICO along with the model estimates and the test data. From the EINO$_x$ figure it is clear that the BM2 does not model the operating conditions between approach and climb-out (which includes the cruise power setting) as well as the physics-based emissions model. The physics-based emissions model's ability to capture the effects of operating conditions on NO_x

emissions makes it a more suitable model in this case for estimating the impact of aircraft operations than the BM2. The EICO figure shows that the physics-based emissions model and the BM2 both estimate the correct trend of EICO with increasing fuel flow rate.

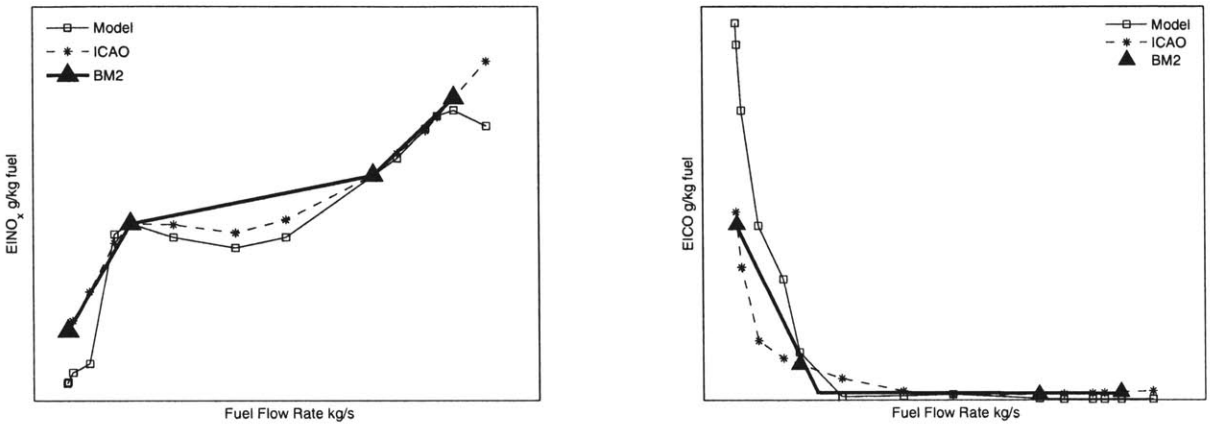

(a) EINO$_x$ (b) EICO

Figure 5-8: Throttle Sweep Emissions Estimates for Engine 1a Compared with Boeing Fuel Flow Method 2

Chapter 6

Conclusions and Future Work

6.1 Conclusions

The objective of this thesis was to create a physics-based emissions model for predicting emissions of potential future gas turbine combustors within quantified uncertainty bounds. To make a successful emissions model for a policy making tool, the model was required to capture the physical relationships among operating conditions, simplified combustor design parameters, and pollutant emissions in a consistent way with one modeling methodology. It was desired first that the model predict the correct sign for changes in emissions with changes in design and operating conditions and if successful, to then predict changes in emissions with changes in design and operating conditions with an accuracy that approaches that of the uncertainty and variability of measurements of emissions indices for the active fleet. The model presented in this thesis did not meet all of the objectives but several important contributions to NO_x and CO emissions modeling were made.

NO_x Emissions

The success criteria for predicting NO_x emissions with the physics-based emissions model was to estimate NO_x emissions within the uncertainty in the certification data or as well as an established empirical model if neither model estimates the emissions levels within the certification data uncertainty. If the physics-based emissions model

could make estimates within the uncertainty in the data or as well as an empirical model while using high-level physical parameters that may be used to project future technologies, then the physics-based model would make a significant contribution to emissions modeling for a policy-making tool.

The result of this work was the creation of a physics-based emissions model that estimated NO_x emissions as well as, or better than, the empirical model at all four certification points for all of the engines and design changes studied in this thesis. The model has the ability to consistently capture the relationships between operating conditions and NO_x emissions as shown in the throttle sweep analysis, and the model has the ability to consistently capture the relationships between combustor design parameters and NO_x emissions as shown by the estimates for Engines 1, 2, and 3. The ability to use one methodology to estimate broad trends in combustor designs for NO_x emissions across engine manufacturers was not studied since only one engine manufacturer was engaged in this research. However, the model was shown to have the ability to use one methodolgy to estimate broad trends in combustor designs within a single engine family as shown by the design change analyses for Engines 1a and 1 and Engines 3 and 3a. The model was also shown to perform better than BM2 for interpolating between certification points.

The only concern regarding the physics-based emissions model's NO_x emissions estimates is that the model does not estimate low power emissions well. The estimates for these cases were usually outside of the uncertainty in the data and the result was that the Dp/Foo estimates for NO_x emissions were not as good as the empirical model estimates for some cases. The empirical model also did a poor job estimating low power NO_x emissions but the errors in emissions estimates at the four certification points for the empirical model often cancelled out when the Dp/Foo was calculated.

Though the model did not strictly meet the objective of predicting NO_x emissions as well as an empirical model, the model did perform better than the empirical model. The inability to correctly capture the change in NO_x Dp/Foo for the two design changes studied in this thesis was due only to poor idle NO_x estimates. The physics-based model has the ability to predict the emissions of a single annular gas turbine

combustor at specific operating conditions using high-level parameters as well as, and in most cases better than, an empirical model. This is a significant contribution to NO_x emissions modeling capability.

CO Emissions

The success criteria for predicting CO emissions with the physics-based emissions model was to estimate CO emissions within the uncertainty in the ICAO certification data. There were no non-proprietary CO emissions models to use to compare how well the model estimates CO emissions to other techniques, so using the uncertainty in the certification data was the only means of assessing the models predictive capability. Because there were no CO emissions models to compare the physics-based emissions model estimates to, the ability to capture the relationships between operating conditions, combustor design parameters, and pollutant emissions consistently, meaning the ability to predict the correct trends in CO emissions with changing conditions and design parameters, would be a significant contribution, even if the model could not estimate the emissions of CO within the uncertainty in the data.

The results presented in this work show that the physical relationships among operating conditions, high-level design parameters, and CO emissions are captured correctly. The response of CO to design parameters like temperature and pressure, as shown in Chapter 4, is captured correctly. The response of CO to changing operating conditions, as shown in the full throttle sweep analysis of Engine 1a, is captured correctly. The changes in CO Dp/Foo that resulted from the design changes from Engine 1a to 1 and Engine 3 to 3a were captured within the uncertainty in the certification data by the model. For most cases, the low power CO emissions, which are more significant than the high power CO emissions because of their contributions to the Dp/Foo, were estimated within the uncertainty in the data.

A concern regarding the CO emissions estimates from the physics-based model is that for Engine 1a, the model did not estimate idle CO within the uncertainty in the certification data. This led to an esitmate of the idle CO for Engine 1 outside of the uncertainty in the data when the design change from Engine 1a to Engine 1

was studied. The result was that the CO estimates of the Dp/Foo values for each engine were not within the uncertainty in the data, which means that the objective of predicting CO emissions within the uncertainty was not met. The poor result may have been the result of an incomplete intermediate zone model for CO emissions predictions and should be looked at in more detail in the future.

Though the model did not meet all the objectives for CO emissions prediction accuracy, it did meet the objective of capturing the physical relationships among operating conditions, design parameters, and CO emissions. A non-proprietary CO emissions model now exists as a result of this work, which is a significant contribution to CO emissions modeling capability.

6.2 Future Work

Although this thesis made contributions to NO_x and CO emissions modeling for policy-making tools, the work is not done. There are several issues that should be explored further. These are the inability to predict CO emissions within the uncertainty in the data for Engine 1a, the poor low power NO_x predictions, the extension of the model to other combustor designs and manufacturing companies, and the develepement of an addition to the model to enable the prediction of soot formation. For CO emissions, different reactor arrangements, particularly for the intermediate zone should be studied. For low power NO_x emissions, different kinetic mechanisms should be studied to determine whether or not poorly modeled low temperature NO_x chemistry is the cause of the erroneous predictions at low power.

If the objectives of this thesis can be met by modifying the reactor arrangement and the kinetic mechanism, then the application of the model to other engine lines and engine manufacturers should be studied. The physics-based emissions model presented in this thesis was designed for single annular combustors and tested with data from one engine manufacturer and one engine line. If the model is to be used in a policy making tool it must be tested across engine manufacturers and across all power levels. New models should also be created, using the same methods developed in this

thesis, for more advanced combustor layouts such as dual-annular combustors, rich-quench-lean combustors, and lean-premix-prevaporize combustors, so that a broader range of potential future technologies may be captured.

Bibliography

[1] The Boeing Company, "Boeing Current Market Outlook 2005," http://www.boeing.com/comerical/cmo.

[2] P.D. Norman, D.H. Lister, M. Lecht, P. Madden, K. Park, O. Penanhoat, C. Plaisance, K. Renger, "Development of the technical basis for a New Emissions Parameter covering teh whole AIRcraft operation: NEPAIR, Final Technical Report," CAEP/6-IP/17 Appendix B.

[3] J.J. Lee, S.P. Lukachko, I.A. Waitz, A. Schafer, "Historical and Future Trends in Aircraft Performance, Cost, and Emissions," Annu. Rev. Energy Environ. 2001, 26:167-200.

[4] N.E. Antoine, I.M. Kroo, "Aircraft Optimization for Minimal Environmental Impact," AIAA 2002-5667.

[5] H. Mongia and W. Dodds, "Low Emissions Propulsion Engine Combustor Technology Evolution Past, Present and Future," GE Aircraft Engines, Cincinnati, Ohio, U.S.A.

[6] Personal Communication with Professor Ian Waitz, MIT, March 2006.

[7] U.S. EPA, "Evalutation of Air Pollutant Emissions from Subsonic Commericial Jet Aircraft," EPA 420-R-99-013 April 1999.

[8] P.J. Jeanniot, "Environmental Review," International Air Transport Association, ISBN 92-9035-732-0.

[9] Intergovernmental Panel on Climate Change, *Aviation and the Global Atmosphere,* Cambridge University Press, 1999.

[10] J.E. Green, "Greener by Design: The Technology Challenge," The report by the Technology Sub Group, Aero Journal, February 2002.

[11] Numerical Propulsion System Simulation tool, NASA Glenn.

[12] Baughcumb, S. L., S. C. Henderson, and T. G. Tritz. "Scheduled Civil Aircraft Emission Inventories for 1976 and 1984: Database Development and Analysis," NASA CR-4722, 1996.

[13] A.M. Mellor and R.M. Washam, "Characteristic Time Correlations of Pollutant Emissions from an Annular Gas Turbine Combustor," Journal of Energy, Vol. 3, No. 4, Article 79-4135, July-August 1979.

[14] A.W. Lefebvre, *Gas Turbine Combustion,* McGraw-Hill 1983.

[15] M.G. Turner, A. Norris, J.P. Veres, "High Fidelity 3D Simulation of the GE90," AIAA 2003-3996.

[16] Gregory P. Smith, David M. Golden, Michael Frenklach, Nigel W. Moriarty, Boris Eiteneer, Mikhail Goldenberg, C. Thomas Bowman, Ronald K. Hanson, Soonho Song, William C. Gardiner, Jr., Vitali V. Lissianski, and Zhiwei Qin, "GRI mech 3.0," http://www.me.berkeley.edu/gri-mech/.

[17] Stephen R. Turns, *An Introduction to Combustion: concepts and applications,* The McGraw-Hill Companies, Inc. 2000.

[18] A. Ghoniem, *Combustion Fundamentals and Applications, Course Notes,* Ghoniem 2005.

[19] G.J. Sturgess, J. Zelina, D.T. Shouse, W.M. Roquemore, "Emissions Reduction Technologies for Military Gas Turbine Engines," Journal of Propulsion and Power, Vol. 21, No.2, March-April 2005.

[20] J.J. Lee, "Modeling Aviation's Global Emissions, Uncertainty Analysis, and Applications to Policy," PhD Thesis, Massachusetts Institute of Technology, 2004.

[21] Personal communication with Dr. Frank Lastrina, GEAE, 2005.

[22] J.B. Moss, *Gas Turbine Pollutant Emissions: Predictive methods for gas turbine combustor emissions*, IMECHE Seminar Publications 2001.

[23] E.M. Greitzer, C.S. Tan, M.B. Graf, *Internal Flow: Concepts and Applications*, Cambridge University Press 2004.

[24] N.K. Rizk, J.S. Chin, A.W. Marshall, M.K. Razdan, "Predictions of NO_x Formation Under Combined Droplet and Partially Premixed Reaction of Diffusion Flame Combustors," Journal of Engineering for Gas Turbines and Power, January 2002, Vol. 124.

[25] C.J. Mordaunt, *Combustion Instability in Land Based Gas Turbines,* www.personal.psu.edu/faculty/c/x/cxm283/research/GTI/stoichiometric_combustor.jpg.

[26] Personal Communication with Nan-Suey Liu, NASA Glenn, April 2006.

[27] G.J. Sturgess, "An Account of FuelAir Unmixedness Effects on NO_x Generation in Gas Turbine Combustors," IECEC-98-353, August 1998.

[28] C.K. Westbrook and F.L. Dryer, "Simplified Reaction Mechanisms for the Oxidation of Hydrocarbon Fuels in Flames," Combustion Science and Technology, Vol. 27, 1981.